© 2020. Published by The Company of Biologists Ltd | Development (2020) 147, dev196394. doi:10.1242/dev.196394

RESEARCH ARTICLE

Molecular mechanisms underlying simplification of venation patterns in holometabolous insects

Tirtha Das Banerjee[1,*] and Antónia Monteiro[1,2,*]

ABSTRACT

How mechanisms of pattern formation evolve has remained a central research theme in the field of evolutionary and developmental biology. The mechanism of wing vein differentiation in *Drosophila* is a classic text-book example of pattern formation using a system of positional information, yet very little is known about how species with a different number of veins pattern their wings, and how insect venation patterns evolved. Here, we examine the expression pattern of genes previously implicated in vein differentiation in *Drosophila* in two butterfly species with more complex venation *Bicyclus anynana* and *Pieris canidia*. We also test the function of some of these genes in *B. anynana*. We identify both conserved as well as new domains of *decapentaplegic*, *engrailed*, *invected*, *spalt*, *optix*, *wingless*, *armadillo*, *blistered* and *rhomboid* gene expression in butterflies, and propose how the simplified venation in *Drosophila* might have evolved via loss of *decapentaplegic*, *spalt* and *optix* gene expression domains, via silencing of vein-inducing programs at Spalt-expression boundaries, and via changes in expression of vein maintenance genes.

KEY WORDS: Venation patterning, *Bicyclus anynana*, Decapentaplegic, *Pieris canidia*, *Drosophila melanogaster*, Spalt, Optix

INTRODUCTION

The arrangement of veins (venation pattern) on the wings of insects play a variety of functions in developing as well as adult insects. Veins provide structural support to the wing, and the venation pattern is important for insect flight (Combes, 2003). Veins also provide nutrients to the developing wing (Chintapalli and Hillyer, 2016) and to live cells in the adult wing, such as pheromone secretory cells (Dion et al., 2016), and even play an auditory function (Sun et al., 2018). The wing veins also play roles in color pattern development, which is involved in sexual and natural selection of many insects such as butterflies and moths (Koch and Nijhout, 2002). Finally, because venation patterns are extremely conserved within a species, but variable across species, they are used extensively in the identification of insect species (Kaba et al., 2017).

Current venation patterns in several insect groups appear to be simplified versions of more complex ancestral patterns. The fossil record indicates that ancestral holometabolous insects, such as *Westphalomerope maryvonneae*, had highly complex vein arrangements that evolved into simpler venation with enhanced efficiency to sustain powered flight in modern representatives of Diptera and Lepidoptera (Nel et al., 2007). To identify these simplifications, Comstock and Needham developed a system of vein homologies across insects in the 1900s (Figs S1 and S2). The system nomenclature recognizes six longitudinal veins protruding from the base of the wings called costa (C), sub-costa (Sc), radius (R), media (M), cubitus (Cu) and anal (A) (Comstock and Needham, 1898). These veins can later branch into smaller veins, and additional complexity is added with cross-veins connecting two or more longitudinal veins. Every longitudinal vein across insects, however, can be identified using this nomenclature. Vein simplifications over the course of evolution have happened either via fusion of veins or disappearance of specific veins (Bier, 2000; De Celis and Diaz-Benjumea, 2003; Garcia-bellido and De Celis, 1992; Stark et al., 1999), but the molecular mechanisms behind these simplifications remain unclear.

Molecular mechanisms of vein pattern formation have been primarily investigated in the model fruit fly *Drosophila melanogaster*, where a classic system of positional information takes place (Fig. S3). Here, the wing is initially sub-divided into two domains of gene expression: an anterior compartment expressing *cubitus-interruptus* (*ci*); and a posterior compartment expressing *engrailed* (*en*) and *invected* (*inv*). In the posterior compartment, *en* and *inv* activate the short-range morphogen *hedgehog* (*hh*) and restrict the activation of *ci* to the anterior compartment. In the anterior compartment, *ci* encodes the protein involved in the transduction of Hh signaling (Cheng et al., 2014; Guillén et al., 1995). Hh diffusing to the anterior compartment establishes a central linear morphogen source of the protein Decapentaplegic (Dpp) at the posterior border of the anterior compartment, and genes like *aristaless* (*al*), *optix*, *spalt* (*sal*) and *optomotor-blind* (*omb*) respond to a Dpp morphogen gradient in a threshold-like manner, creating sharp boundaries of gene expression that provide precise positioning for the longitudinal veins (Barrio and De Celis, 2004; Martín et al., 2017; Sturtevant et al., 1997). Veins differentiate along these boundaries, along a parallel axis to the Dpp morphogen source via activation of vein-specific genes such as *knirps* (*kni*), *knirps-related* (*knil*) and *abrupt* (*abt*) (Blair, 2007; De Celis, 2003; Martín et al., 2017). Vein cell identity is later determined by the expression of genes such as *rhomboid* (*rho*), which is downstream of the aforementioned genes (Guichard et al., 1999; Sturtevant et al., 1997). Conversely, intervein cells will later express *blistered* (*bls*), which suppresses vein development (Fristrom et al., 1994; Roch et al., 1998). The final vein positions are then determined by the cross-regulatory interaction of *rho* and *bls*.

The mechanisms underlying venation patterning in other insect lineages have remained poorly understood; so far, gene expression patterns and functions for the few genes examined in beetles (order Coleoptera), ants (order Hymenoptera) and scuttle flies (order Diptera) seem to be similar to those in *Drosophila* (Abouheif and Wray, 2002; Gantz, 2015; Tomoyasu et al., 2005; Wang et al., 2017).

[1]Department of Biological Sciences, National University of Singapore, 117557 Singapore. [2]Yale-NUS College, 138527 Singapore.

*Authors for correspondence (tirtha_banerjee@u.nus.edu; antonia.monterio@nus.edu.sg)

T.D.B., 0000-0002-6092-0824

Handling Editor: Cassandra Extavour
Received 27 August 2020; Accepted 21 October 2020

Development (2020) 147, dev196394. doi:10.1242/dev.196394

Venation patterning in butterflies (order Lepidoptera) has been examined in a few mutants in connection with alterations of color pattern development (Koch and Nijhout, 2002; Schachat and Brown, 2015) and more directly via the expression pattern of a few genes during larval development. Two of the species in which a few of the venation patterning genes have been studied in some detail are the African Squinting Bush Brown butterfly, *Bicyclus anynana*, and the common Buckeye butterfly, *Junonia coenia*. In both species, En and/or Inv were localized in the posterior compartment using an antibody that recognizes the epitope common to both transcription factors (Keys et al., 1999; Monteiro et al., 2006). The transcript of *inv* in *Junonia*, however, appears to be absent from the most posterior part of the wings (Carroll et al., 1994), whereas the transcript of *hedgehog* (*hh*), a gene that is upregulated by En/Inv in *Drosophila* (Tabata et al., 1992) is uniformly present in the posterior compartment of both species (Keys et al., 1999; Saenko et al., 2011). Little is known of the expression domains of the other genes, including the main long-range morphogen *dpp* and its downstream targets [e.g. *sal*, *aristaless* (*al*), *optomotor blind* (*omb*) and *optix*] with respect to venation patterning. Studies on *optix* have been mostly focused on understanding the mechanisms underlying color pattern development during the late pupal stages (e.g. its role in the development of red pattern elements in *Heliconius* butterflies) (Jiggins et al., 2017; Reed et al., 2011; Zhang et al., 2017). Al has also been proposed to play a role in color pattern development in *J. coenia* and *Heliconius* butterflies, in particular in the coloring of transverse bands (Martin and Reed, 2010; Westerman et al., 2018). A recent report proposed the presence of a second *dpp*-like organizer at the far posterior compartment in butterflies (Abbasi and Marcus, 2017). This report, however, showed no direct gene expression or functional evidence, and has been debated by other researchers (Lawrence et al., 2017). Currently, there is also no functional evidence of altered venation for knockout phenotypes for any of these genes in Lepidoptera.

In the present work, we explore the expression of an orthologous set of genes to those that are involved in setting up the veins in *Drosophila* in two butterfly species: *Bicyclus anynana* and *Pieris canidia*. We subsequently perform CRISPR-Cas9 and drug inhibition experiments to test the function of some of these genes in venation patterning in *B. anynana*.

RESULTS

Staging of the butterfly wings

Comparative analysis between two distantly related butterfly species, with different larval and pupal development times, as well as with *Drosophila*, with three larval instars instead of the five observed in butterflies requires an initial consideration of what might be comparable wing developmental stages for vein differentiation. Age of larvae (e.g. days since last molt) is a poor predictor of the development state of the wings in butterflies (Reed et al., 2007). Wing development of butterflies in the larval stage involves the growth and expansion of a flattened wing disc, with a ventral and dorsal layer of cells on each side of the disc. This arrangement of cells is unlike that of *Drosophila*, where the wing blade during the larval stage has a single sheet of cells that later folds to become the dorsal and ventral surface. Wing discs in both *Bicyclus* and *Pieris* remain very small until the final (fifth) instar. The same is true for larval wing discs of *Drosophila* (Matsuda and Affolter, 2017). Based on the onset of the expression of multiple homologous genes, described below, we estimated that venation patterning starts during the final instar of both butterfly and fly wing discs. A previous study described the developmental stages of butterfly wing discs during the final instar using the pattern of tracheal growth as it invades the lacunae, the space between the dorsal and ventral epidermal layers, and zone of differentiation of the future veins (Reed et al., 2007). This study uses a numbering system from 0.00 (wing at the late fourth to beginning of the fifth instar) to 4.00 (wings at the end of the fifth instar, the wandering stage, immediately before the pre-pupal stage) (Reed et al., 2007). Along with the tracheal invasion data, which start at stage 1.00, we used the cellular arrangement and the shape of the wing margin as indicators of developmental stages prior to stage 1.00 (Fig. 1), as mentioned below. We focused most of our analyses on larval wings between developmental stages 0.00 and 1.00, the time we estimated venation patterning is taking place in lepidopteran wings (Fig. 1).

Expression of *engrailed* and *invected* transcripts and proteins

We first examined the expression pattern of En and Inv at both the transcript and protein levels in *B. anynana* and in *P. canidia* fifth instar larval wings. We used an antibody (4F11) that recognizes the epitope of both proteins and confirmed that En and/or Inv expression is found throughout the posterior compartment in both forewings and hindwings in *B. anynana* (Keys et al., 1999; Patel et al., 1989), and also in *P. canidia.* However, a sharp drop in expression levels is observed posterior to the A2 lacuna in both species (Fig. 2A-D). We will use 'vein' instead of lacuna from here onwards, for simplicity, even though at this stage we only observe a pattern of longitudinal gaps between the two layers of wing epidermis and not proper vein tissue. We hypothesized that the low En/Inv posterior expression could be due either to lower levels of transcription or translation of En and/or Inv, or to the absence of either of the two transcripts in the area posterior to the A2 vein. To test these hypotheses, we performed *in situ* hybridization using probes specific to the transcripts of *en* and *inv* in *Bicyclus* (see Table S1). *en* was expressed homogeneously throughout the entire posterior compartment on both the forewing and the hindwing, but *inv* was restricted to the anterior ∼70% of the posterior compartment (Fig. 2E-H). Hence, the low levels of En/Inv protein expression appear to be due to the absence of *inv* transcripts in the most posterior region of the posterior compartment.

Expression and function of *dpp* (BMP signaling)

We explored the presence of transcripts for the BMP signaling ligand Decapentaplegic (Dpp) with the help of *in situ* hybridization using a probe specific to its transcript (see supplementary Materials and Methods for sequence). A band of *dpp* was observed along the A-P boundary (i.e. along the M1 vein) as previously reported by Connahs et al. (2019). However, another expression domain was observed in the lower posterior compartment around the A3 vein (Fig. 3A; Fig. S4A-C). Inhibiting BMP (Dpp) signaling via Dorsomorphin resulted in the reduction of overall wing size (Fig. 3D; Fig. S4E), and in incomplete and ectopic development of veins, indicating a role for Dpp in wing growth and vein development (Fig. 3E-G). Furthermore, disrupting *dpp* via CRISPR-Cas9 resulted in ectopic and missing vein phenotypes emerging from the Cu2 and Cu1 veins (Fig. 3H; Fig. S4H). Inhibition of BMP signaling by Dorsomorphin also resulted in reduced transcription of *spalt* during larval wing development, a known downstream target of Dpp signaling in *Drosophila* wings (Blair, 2007; Szuperak et al., 2011) (Fig. 3I).

Expression and function of *spalt*

To localize the transcription factor Sal (only one *spalt* gene is present in *Bicyclus*; Nowell et al., 2017) we performed immunostaining in larval wings of *B. anynana* and *P. canidia*

Development (2020) 147, dev196394. doi:10.1242/dev.196394

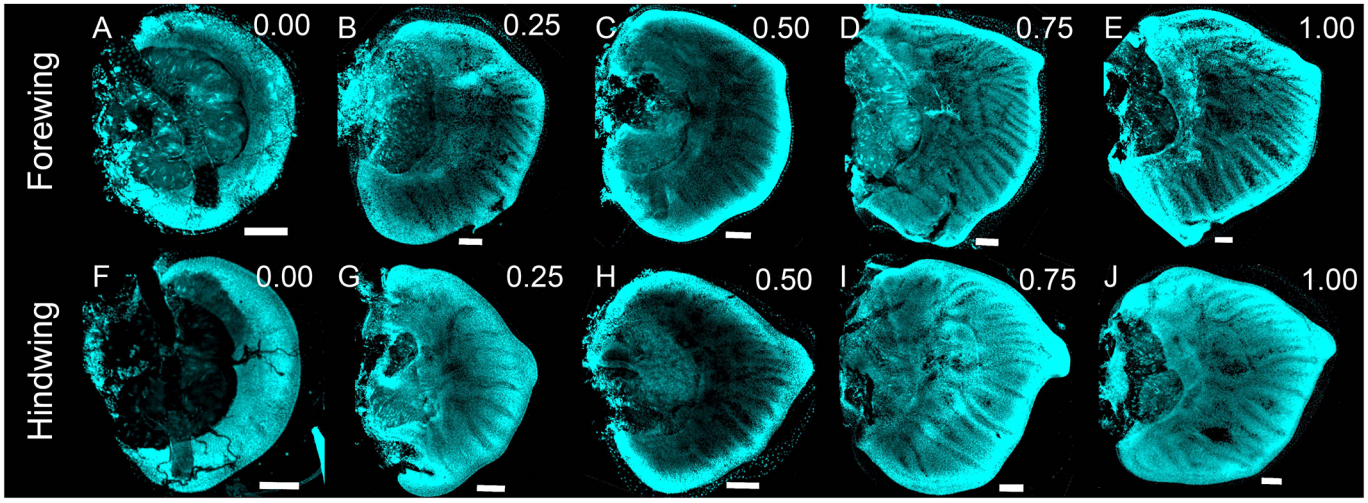

Fig. 1. DAPI staining and staging of early larval wing development of *Bicyclus anynana*. Staging is based on work by Reed et al. (Reed et al., 2007), and on cellular arrangements and wing shape changes. (A-E) Forewings. (F-J) Hindwings. (A,F) Stage 0.00 is the earliest stage at which wing staining is possible at the end of the fourth instar. The wing disc is crescent shaped, surrounding a mass of central cells. Epidermal cells are homogenously distributed and it is difficult to distinguish forewings and hindwings based on morphology. (B,G) Stage 0.25 is when the wing starts to develop a slight bulge at the distal edge. Cell density is higher along the wing margin and lower along the position of the future veins. These areas, also called lacuna, represent areas through which the tracheal system will invade, in between the dorsal and ventral surfaces, and that will differentiate into veins. (C,H) Stage 0.50. Cell density increases in the wing margin and the fore- and hindwings can be distinguished on the basis of their shape. (D,I) Stage 0.75. The wing is much larger compared with the previous stage and exhibits higher density of cells in the wing margin and flanking the lacuna. (E,J) Stage 1.00. The cells continue to condense around the veins/lacuna and tracheal invasion starts to happen. Scale bars: 100 µm.

using an antibody previously described (Stoehr et al., 2013). Sal is expressed in four clearly separated domains in both early (0.25) and later (1.00) stages of development (Fig. 3K-P; Fig. S5B,D,F). The first domain is anterior to the Sc vein. The second domain spans the interval between the R2 and M3 veins. The third domain is between the Cu2 and A2 veins. No expression is observed between the A2 vein and a boundary between the A2 and A3 veins; and finally, a fourth domain is present posterior to the boundary between the A2 and A3 veins (Fig. S5H). These expression domains are also observed in *P. canidia* (Fig. 3Q,R).

To test the function of *sal* in vein development, we targeted this gene using CRISPR-Cas9. The phenotypes observed support a role for *sal* in establishing vein boundaries at three out of the four domains described above (Fig. 3K-P). We observed both ectopic and missing vein phenotypes in both the forewing and the hindwing at the domains where Sal protein was present during the larval stage

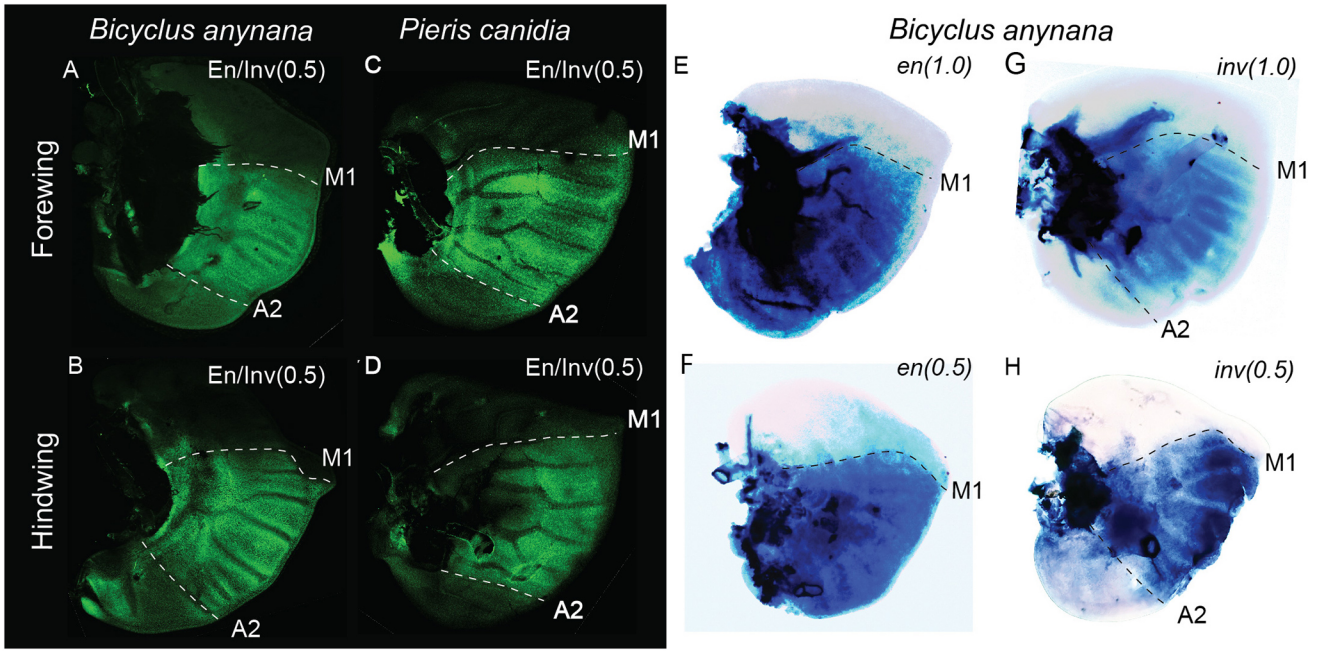

Fig. 2. Expression of Engrailed and Invected proteins in *Bicyclus anynana* and *Pieris canidia*, and expression of mRNA transcripts in *Bicyclus anynana* larval wings. (A-D) Expression of En/Inv proteins in the larval forewing (A) and hindwing (B) of *B. anynana*, and forewing (C) and hindwing (D) of *P. canidia* is strong between the M1 and A2 veins, and weaker posterior to the A2 vein. (E,F) Expression of *en* mRNA transcripts in the forewing (E) and hindwing (F) in *B. anynana* is almost homogeneous across the posterior compartment. (G,H) Expression of *inv* in the forewing (G) and hindwing (H) in *B. anynana* is detected in around 70% of the posterior compartment from the M1 vein to the A2 vein.

Development (2020) 147, dev196394. doi:10.1242/dev.196394

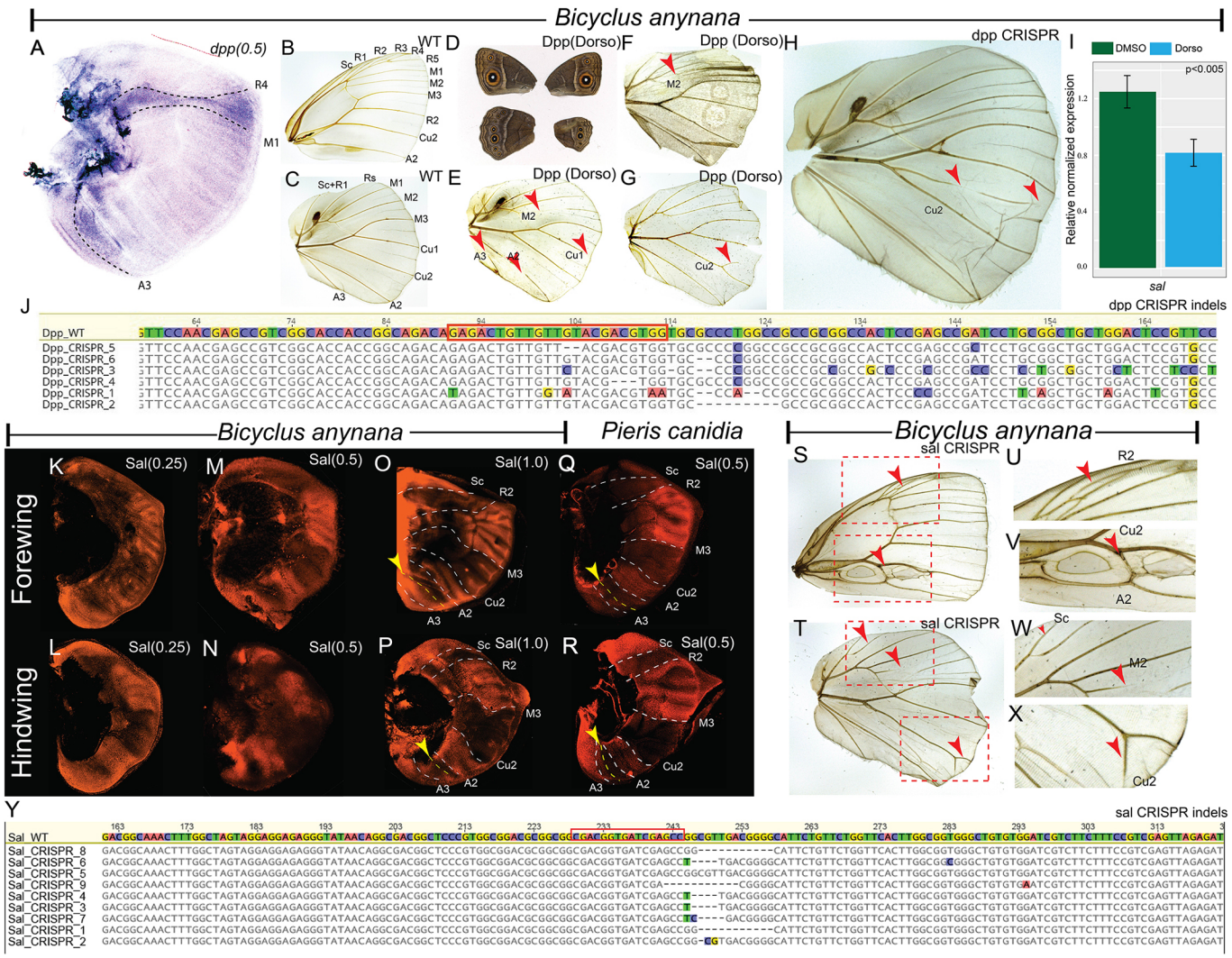

Fig. 3. Expression and function of *dpp* and *sal* in *Bicyclus anynana*, and expression of *sal* in *Pieris canidia*. (A) Expression of *dpp* in the larval wing of *B. anynana* is visible anterior to the A-P boundary (M1), in between the R4 and M1 veins (for vein positioning at the same stage, refer to Fig. S2), and around the A3 vein. (B,C) Wild-type adult forewing (B) and hindwing (C). (D) The hindwing of an adult individual treated with dorsomorphin (on the right) showing a reduction in size. (E,F) Dorsomorphin-treated wings also fail to form complete veins such as the M2, Cu1, A2 and A3 veins (E, red arrowheads), and the M2 vein (F, red arrowhead). (G) Dorsomorphin treatment also produces ectopic veins at Cu2 (red arrowhead). (H) A *dpp* crispant produced ectopic and missing vein phenotype (red arrowheads) at Cu2. (I) *sal* qPCR on dorsomorphin-treated wings. The levels of *sal* transcripts are reduced due to BMP inhibition. Error bars indicate s.d. (J) Indels at the *dpp* CRISPR-Cas9 cleavage sites (red rectangle) obtained from the wing in H. (K-P) Expression of Sal in larval forewings at stages (K) 0.25, (M) 0.5 and (O) 1.0, and in larval hindwings at stages (L) 0.25, (N) 0.5 and (P) 1.0, showing four distinct domains of expression: from the anterior margin to the Sc vein; from the R2 to M3 vein; from the Cu2 to A2 vein; and from a boundary in between the A2 and A3 veins to the posterior wing margin. The yellow dotted lines and arrowheads indicate the upper boundary of the fourth Spalt expression domain. (Q,R) Expression of Sal in the larval forewing (Q) and hindwing (R) of *P. canidia*. (S-X) In CRISPR-Cas9 *sal* crispants, ectopic veins (red arrowheads) are produced within the boundaries of Sal expression in forewings (S,U,V) and ectopic, as well as missing veins (red arrowheads), are produced within the Sal expression domains in hindwings (T,W,X) (descaled adult wings). (Y) Indels at the *sal* CRISPR-Cas9 cleavage sites (red rectangle) obtained from the wing in S.

of wing development (Fig. 3S-X; Fig. S5M-X). In the forewing, *sal* crispants generated ectopic and loss of vein phenotypes between the R2 and the M3 vein domain (Fig. 3S,U; Fig. S5O,U,W), and ectopic veins between the Cu2 and A2 veins (Fig. 3S,V; Fig. S5M,Q-W). In the hindwing, we observed ectopic veins connecting to the existing Sc vein (Fig. 3T,W; Fig. S5X), missing veins between the Rs and M3 vein (Fig. 3T,W; Fig. S5N,P,R), and ectopic veins between the Cu2 and A2 veins (Fig. 3T,X; Fig. S5T,V).

Expression and function of *optix*

Optix proteins are present in two domains during early larval wing development. Anterior to the R2 vein (Rs for hindwing) and posterior to the A2 vein (Fig. 4;Fig. S6A,C,E). Optix is also present in scale cells involved in orange pigment production in later (pupal) stages of wing development (Fig. S6R). Knocking out *optix* using CRISPR-Cas9 resulted in the loss of these orange scales (Fig. S6M-Q), but no changes in venation were observed (Fig. S6K,L).

Expression and function of *wg* (Wnt signaling)

During the early larval wing development (0.5) *wg* is expressed along the wing margin (Fig. 5A,B; Fig. S7A-C). At an earlier stage (0.25), the signal transducer of Wg signaling, Armadillo (Arm), has a homogeneous expression across the wing disc (Fig. 5C,D). Later in development, at stage 1.0, Arm shows more focused expression in the

Development (2020) 147, dev196394. doi:10.1242/dev.196394

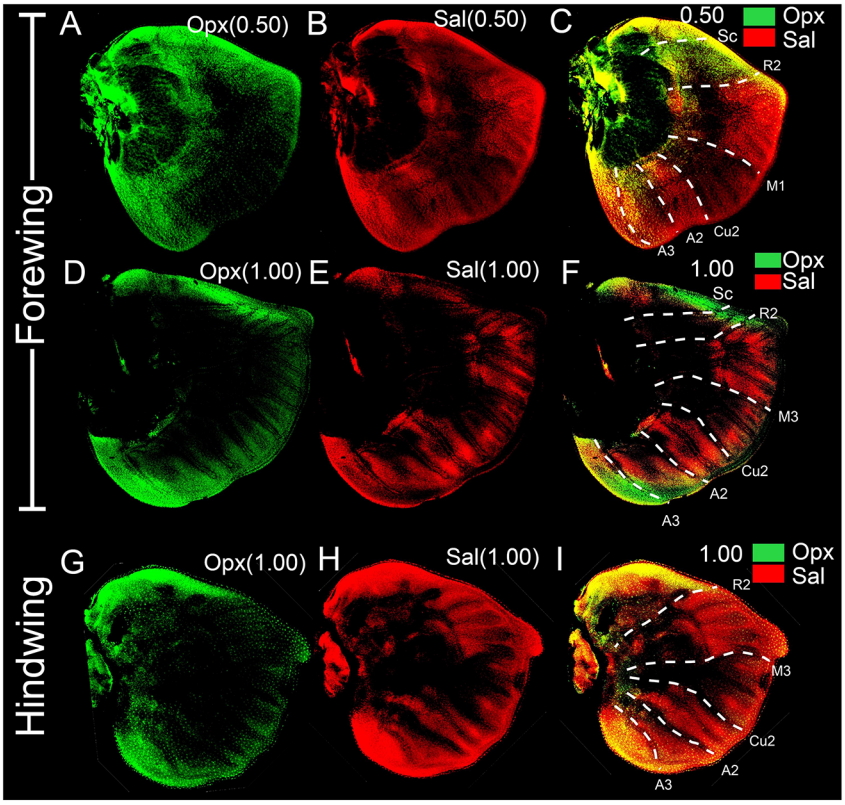

Fig. 4. Expression of Optix (Opx) and Spalt (Sal) in *Bicyclus anynana* larval wings. (A,D,G) Double immunostaining shows expression of Optix proteins in the larval forewing (A,D) and hindwing (G). Optix expression is stronger in two regions: one anterior to the R2 vein and one posterior to the A2 vein (stage 0.5 and 1.0). (B,E,H) Expression of Spalt in the same wings. (C,F,I) Merged channels of Opx and Sal.

wing margin, at the eyespots centers and mid-line connecting these centers to the wing margin, and along the veins (Fig. 5E,F). Inhibition of Wnt signaling using the small drug inhibitor iCRT3 (Lee et al., 2013) led to the reduction of wing size; however, no defects in the veins were observed (Fig. 5G-I; Fig. S7E,F).

Expression of *blistered* (*bls*) and Rhomboid (Rho)

To localize vein and intervein cells, we performed *in situ* hybridization of the intervein marker and vein suppressor gene *bls*, and antibody stains against the vein marker and vein promotor gene Rho. In the larval forewing and hindwing of *B. anynana*, *bls* is expressed in the intervein cells and is absent in the vein cells and cells around the wing margin (Fig. 6A-D; Fig. S7G-I). During an early developmental stage (0.5), *bls* is absent in the A1 vein (Fig. 6A,B; Fig. S7G), however, later in development stage 1.75, *bls* moves into the A1 vein (Fig. 6C,D; Fig. S7H,I).

An antibody raised against *B. anynana* Rho (an intramembrane serine protease) showed expression along the veins and around the wing margin (Fig. 6E,F,K-M). A high level of Rho is observed at the A1 vein during an early developmental stage (0.5) (Fig. 6L); however, as the wings develop, the expression at the A1 vein becomes weaker (stage 1.75) (Fig. 6M). During these later stages of development, tracheal tissues move into the veins and these tissues are autofluorescent. The fluorescence is removed during image acquisition as observed in Fig. 6M (trachea appear dark). The levels of Rho are still higher at the location of the veins, as observed in the Cu2 vein just above the A1 vein in Fig. 6M, where the trachea has not invaded yet. The expression of Rho is complementary to that of *bls*.

DISCUSSION

A positional-information mechanism like that observed in *Drosophila* appears to be involved in positioning the veins in *B. anynana* and *P. canidia*; however, differences exist between flies and butterflies at multiple stages of vein patterning (Fig. 7). These differences are highlighted below.

The early wings of *B. anynana* are subdivided into three gene expression domains instead of two, as in *D. melanogaster*

One of the earlier steps in vein patterning in *D. melanogaster* is the separation of the wing blade into distinct compartments via the expression of En/Inv in the posterior compartment (Fig. 7D) (Guillén et al., 1995). *In situ* hybridization against the separate transcripts of *en* and *inv* in *B. anynana*, showed that *en* is expressed across the whole posterior compartment (in the whole region posterior to the M1 vein) and continues until the pupal stage (Banerjee et al., 2020), as in *D. melanogaster* (Blair, 1992), whereas *inv* is expressed only in the most anterior region of the posterior compartment, anterior to the A2 vein. This presumably leads to the higher En/Inv protein levels observed in the upper posterior compartment, and lower protein levels in the lower posterior compartment (Fig. 7I). Although the *en in situ* results are new, the *inv* expression is consistent with that observed in a previous study by *J. coenia* (Carroll et al., 1994). The *inv* expression pattern in butterflies is, thus, distinct from that of *D. melanogaster* where *inv* is expressed homogeneously throughout the posterior compartment (Cheng et al., 2014). These differences in expression of *en* and *inv* between *D. melanogaster* and *B. anynana* essentially set up two main domains of gene expression in fly wings but three in butterfly wings: an anterior domain with no *en* or *inv* expression; a middle domain with both *en* and *inv*; and a posterior domain with *en* but no *inv*.

Two *dpp* signaling domains are established in *B. anynana*, whereas a single domain is present in the wing pouch of *D. melanogaster*

The next step in venation patterning in *D. melanogaster* is the establishment of the main *dpp* organizer along a stripe of cells, in the middle of the wing pouch (Tanimoto et al., 2000). This group of

Development (2020) 147, dev196394. doi:10.1242/dev.196394

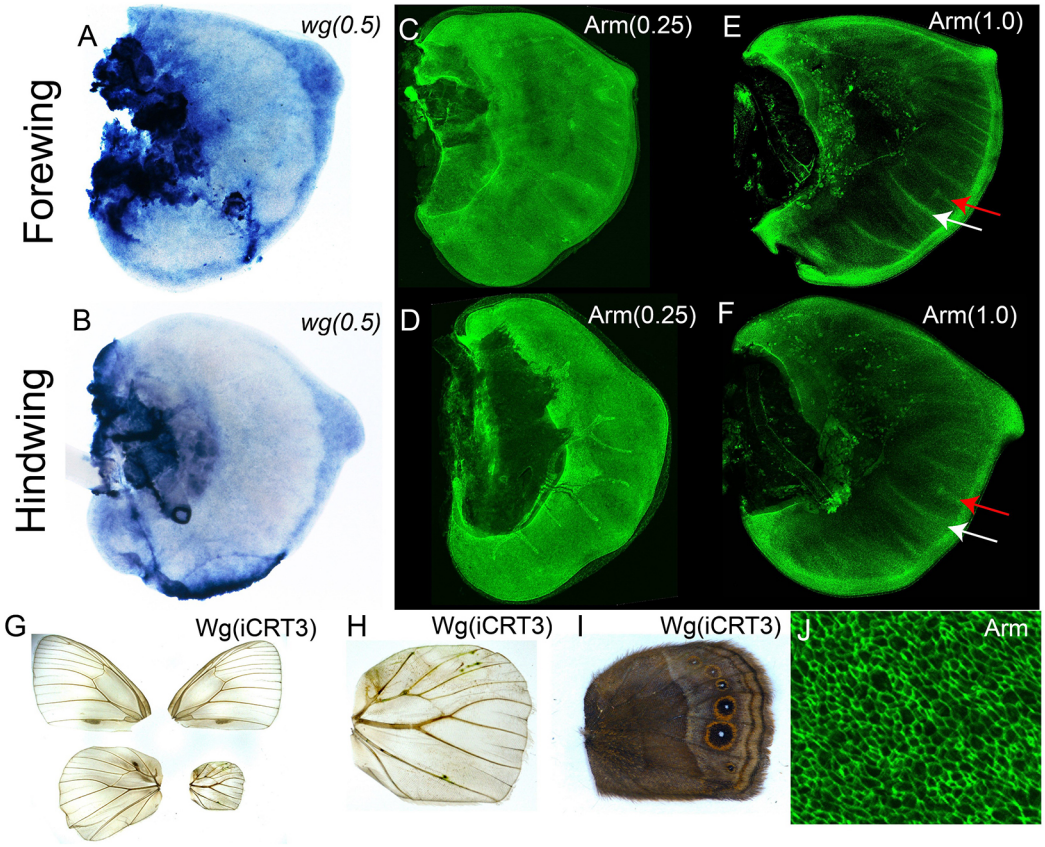

Fig. 5. Expression of *wingless* (*wg*) and Armadillo (Arm), and the function of Wnt signaling in *Bicyclus anynana*. (A,B) *wg* is expressed in the wing margin at the 0.5 stage in larval wings. (C-F) Expression of Arm during different larval developmental stages. During (C) early forewing and (D) early hindwing development, Arm is more homogeneously expressed; during later stages of development in both the (E) forewing and (F) hindwing, expression is stronger in the wing margin, along the veins (white arrows) and in the eyespot centers (red arrows). (G,H) An individual treated with the Wnt inhibitor iCRT3 shows (G) reduction in the size of its hindwing (which was next to the site of injection) but (H) no effect in the venation of the wing (descaled hindwing). (I) Same wing as in H, before descaling. Eyespots became reduced in proportion to wing size due to Wnt inhibition. (J) Higher-magnification image of Arm expression in the larval wing at the 0.25 stage.

dpp-expressing cells is established just anterior to the *en/inv*-expressing cells, at the A-P boundary, where the M1+2 (L4) vein will differentiate (Ingham and Fietz, 1995; Tanimoto et al., 2000). The R4+5 (L3) vein differentiates at the anterior boundary of *dpp*-expressing cells due to activation of Epidermal Growth Factor (EGF) signaling via the gene *vein* (*vn*) co-expressed with *dpp* in response to Hh diffusing from the posterior compartment (Bier, 2000; Simcox et al., 1996). In *B. anynana* we also observe a group of cells expressing *dpp* at the A-P boundary anterior to the M1 vein (Fig. 7J). This *dpp* expression in *B. anynana* is likely driven by Hh diffusing from the posterior compartment to the anterior compartment where *Cubitus interruptus* (Ci), the signal transducer of Hh signaling, is present (Keys et al., 1999; Saenko et al., 2011). We propose that the R4 vein forms at the anterior boundary of *dpp*-expressing cells, as it does in *D. melanogaster* (Bier, 2000). In *B. anynana* there is a second group of *dpp*-expressing cells straddling the A3 vein (Fig. 7J). This second *dpp* domain in *B. anynana* is probably activated via a Hh-independent mechanism, as no Ci or Patched (the receptor of Hh signaling) expression is observed in the posterior compartment around the A3 vein in butterflies (Keys et al., 1999; Saenko et al., 2011). In *D. melanogaster,* there is also a group of *dpp*-expressing cells outside the wing pouch, which are activated via a Hh-independent mechanism (Foronda et al., 2009) (Fig. 7E). These two groups of cells could be homologous.

Four domains of Sal expression are established in *B. anynana*, whereas a single domain is present in *D. melanogaster* larval wing pouch

The expression of *dpp* activates the next step in venation patterning in *D. melanogaster*, which involves the activation of *sal* expression some distance away from the signaling center in a single main central domain (Barrio and De Celis, 2004; Bier, 2000; Blair, 2007; Strigini and Cohen, 1999). Here, the anterior boundary of Sal expression is involved in setting up the R2+3 (L2) vein (Bier, 2000; Blair, 2007; Cook et al., 2004; Sturtevant et al., 1997). In *B. anynana*, Sal is expressed in four separate domains in the larval wing, and functional data (discussed below) indicate that the boundaries delimiting the three most anterior Sal domains set up veins Sc, R2, M3, Cu2 and A2 (Fig. 7K). Only two of the Sal domains straddle the two *dpp* expression domains (Fig. 7J,K). This suggests that Dpp might be activating *sal* in two of the domains where *dpp* and Sal are co-expressed and overlap, but some other morphogen might activate *sal* in the first and third domains of Sal expression in *B. anynana*. We explored both the expression and function of Wg, as well as its signal transducer Armadillo (Arm), as possible activators of these additional Sal domains, as discussed in the sections below, but found no supporting evidence for this. In *D. melanogaster*, only one Sal central domain is present in the

Development (2020) 147, dev196394. doi:10.1242/dev.196394

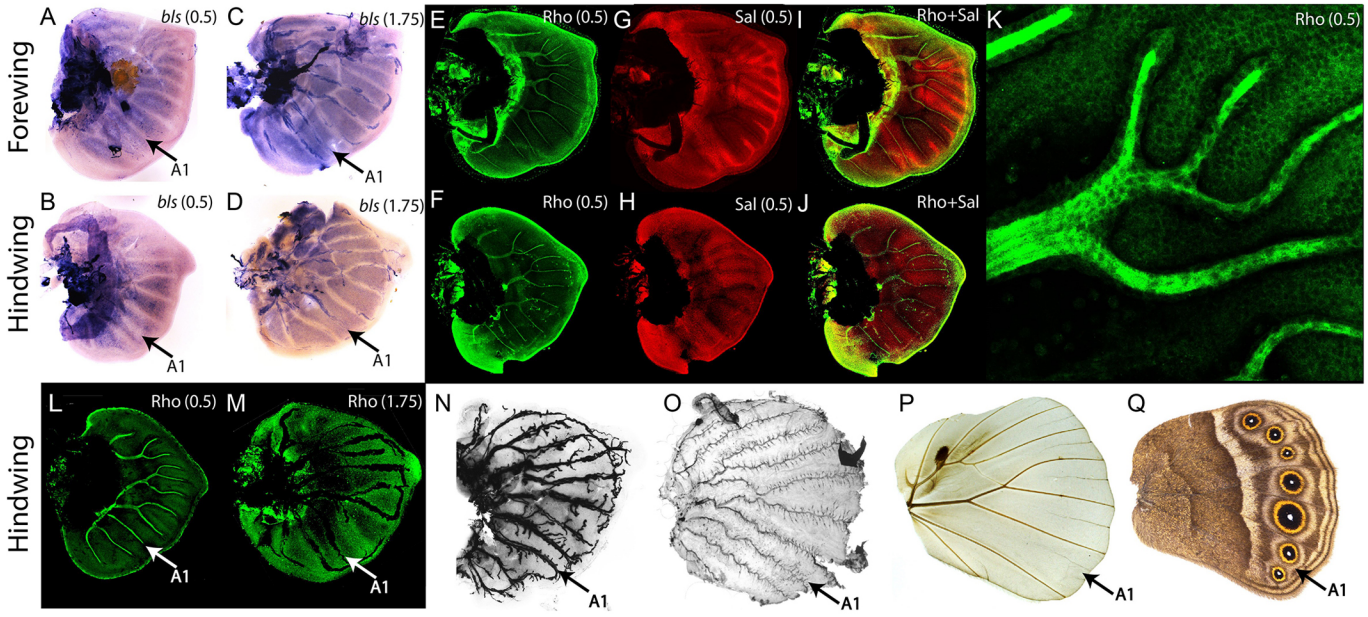

Fig. 6. Expression of *blistered* (*bls*) and Rhomboid (Rho), and loss of the A1 vein in *Bicyclus anynana*. (A,B) Expression of *bls* in the intervein cells during early larval forewing (A) and hindwing (B) stages (0.5). (C,D) During later stages of development, *bls* expression is observed in the A1 vein, which will disappear in the pupal stage. (E,F) Expression of Rho (an intramembrane serine protease) in the larval forewing and hindwing. Rho is expressed along the veins and the wing margin. (G,H) Expression of Sal in the same wings as E,F. (I,J) Merged channels of Rho and Sal expression. (K) High-magnification image of Rho expression. (L) Rho is expressed in vein A1 at stage 0.5. (M) Expression of Rho at stage 1.75. The tracheal cells along the veins at this stage are auto-fluorescent and were removed during image acquisition. A lower amount of signal is obtained from the region around the A1 vein. (N-Q) Disappearance of the A1 vein in *B. anynana* during the pupal to adult wing transition: (N) larval wing; (O) pupal wing; (P) adult wing with scales removed; (Q) adult wing with scales. The A1 vein is observed in the larval and pupal stages, but it disappears in the adult stage.

wing pouch during the larval stage, where venation patterning takes place (circle in Fig. 7F), but a more-anterior and a more-posterior Sal expression domain appear during the pupal stage (Fig. 7H) (Biehs et al., 1998; Grieder et al., 2009; Sturtevant et al., 1997). To our knowledge, no study has yet elucidated which gene drives the expression of Sal in these additional domains in *D. melanogaster* pupal wings.

Two domains of Optix expression are observed in *B. anynana*, whereas a single domain is present in *D. melanogaster*

In *B. anynana*, we observe two expression domains of Optix, one in the upper anterior compartment and one in the lower posterior compartment (Fig. 7K). In *D. melanogaster*, however, only one Optix expression domain is observed in the upper anterior compartment in response to low levels of Dpp secreted from the A-P boundary (Martín et al., 2017; Al Khatib et al., 2017). In *B. anynana*, both Optix domains are also likely activated by Dpp. The upper anterior domain of Optix (Fig. 7K) likely responds to low levels of Dpp secreted from the A-P boundary (Fig. 7J), whereas the lower posterior domain of Optix (Fig. 7K) is likely activated by Dpp present around the A3 vein (Fig. 7J). It is interesting to note that the first and the fourth domains of Sal overlap with the anterior and the posterior domains of Optix, respectively, as Sal has been shown to repress *optix* in its own domain straddling the A-P boundary in *D. melanogaster* (Martín et al., 2017) (Fig. 7K). Co-expression of Sal and Optix at the upper anterior and lower posterior compartment might be an ancestral state that became modified in modern insects. Conserved (from larval stage) and novel expression domains of Optix during the pupal wing stage (T.D.B. and A.M., unpublished) are involved in the development of ommochrome pigments in different areas of the wing (Fig. S6).

sal crispants show that three Sal boundaries are involved in positioning veins in *B. anynana*, whereas a single Sal boundary performs this function in *D. melanogaster*

Sal knockout phenotypes in *B. anynana* led to disruptions of veins in three out of the four Sal expression domains suggesting that, as in *D. melanogaster*, Sal is involved in setting up veins. *sal* crispants displayed: (1) ectopic Sc veins at the posterior boundary of the first Sal expression domain (Fig. 3S,T,W; Fig. S5X); (2) both ectopic and missing veins in the region of the second Sal domain straddling the A-P boundary, on both forewings and the hindwings, consistent with previous results on *Drosophila* (Fig. 3S-V; Organista and De Celis, 2013; Sturtevant et al., 1997); and (3) ectopic veins in both the forewing and the hindwing in the region of the third Sal domain (Fig. 3V,X; Fig. S5S-W). The final Sal expression domain in *Bicyclus* is present posterior to a boundary running between the A2 and A3 vein (Fig. S5H); we obtained no crispant with disruptions in veins in this area. Our data therefore provide evidence that Sal boundaries of expression in domains 1, 2 and 3 are involved in differentiating veins at those boundaries in *B. anynana*, whereas the boundary of the last Sal domain might not be used to position veins in the most posterior wing region (Fig. 7K,L).

The presence of both ectopic veins as well as disrupted veins in the domains of Sal expression in *Bicyclus* might be due to the disruption of the vein-intervein network in those regions. In *D. melanogaster*, ectopic and disrupted veins in *sal* knockout mutants lead to ectopic and missing *rho* expression (Sturtevant et al., 1997). A proposed mechanism for how these genes interact involves Sal, Opx, Aristaless (Al) and Knirps. In *D. melanogaster*, a single stripe of Knirps is present along the R2+3 (L2) vein in response to Dpp signaling. Dpp from the A-P margin activates Al throughout the anterior compartment. *sal* is activated in response to a high concentration of Dpp posterior to the R2+3 (L2) vein and

Development (2020) 147, dev196394. doi:10.1242/dev.196394

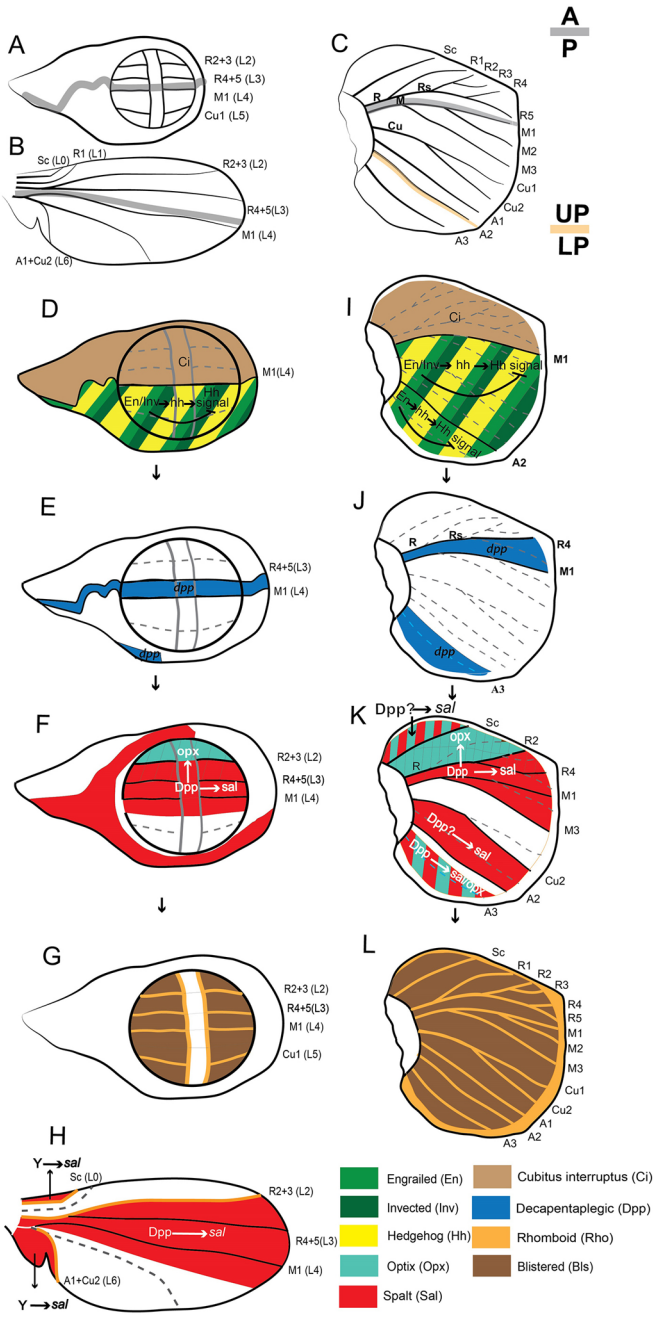

Fig. 7. A model for venation patterning in *Bicyclus anynana* and comparison with *Drosophila melanogaster*. (A,B) Venation in *D. melanogaster* larval (A) and pupal (B) wing. (C) Venation in *B. anynana* larval forewing. The anterior-posterior (A-P) boundary is marked by the thick gray line. The boundary between the upper-posterior gene expression domain (UP, from the M1 to A2 vein) and the lower-posterior gene expression domain (LP, from the A2 vein until the posterior wing margin) of the wing is marked by the thick orange line (drawn based on Methylene Blue staining in Fig. S8). (D-H) Venation patterning in the *D. melanogaster* wing (for details refer to the main text). (I) We propose that, in *B. anynana*, venation patterning is initiated by En and Inv expressed in the posterior compartment. En/Inv or En activates Hh in the posterior compartment, while suppressing Hh signaling. (J) A small amount of Hh diffuses into the anterior compartment where, due to the presence of the Hh signal transducer Ci, it activates *dpp* in a thin stripe of cells between the R4 and M1 veins. The boundary between *dpp*-expressing and non-expressing cells potentially sets up the position of the R4 and M1 veins (as it does in *Drosophila*, E). A second domain of *dpp* is activated straddling the A3 vein via a Hh-independent mechanism. (K) In *B. anynana*, Sal is expressed in four distinct domains and Opx in two distinct domains, in response to Dpp signaling. The three most-anterior domains of Sal are involved in induction of veins at the domain boundaries (Sc, R2, M3, Cu2 and A2). (L) In *B. anynana*, as in *D. melanogaster* (G), Rho is expressed along the veins and *bls* is expressed in the intervein cells.

optix is activated only anterior to the R2+3 (L2) vein in response to presence of Dpp but absence of Sal (Martín et al., 2017). These different expression domains create a perfect environment at the R2+3 (L2) vein where Al activates *knirps*, while Sal and Opx repress *knirps* expression (Martín et al., 2017). Knirps then activates further downstream genes, such as *rho* that induces vein development (Lunde et al., 1998). Our *knirps* staining using *in situ* hybridization and immunostaining (Kosman et al., 1998) did not produced any positive result; however, expression of Sal, Opx and Al (Fig. S6A-H) indicates that a similar mechanism might be in place in *B. anynana*, where the absence of Sal and Opx at the R2 vein might lead to activation of a gene similar to *knirps* by Al present homogeneously in the anterior compartment (Fig. S6G,H).

An alternative mechanism for how these genes interact involves Sal activating a hypothetical short-range diffusible protein in the intervein cells and at the same time inhibiting the intervein cells from responding to the signal (Bier, 2000; Sturtevant et al., 1997). A small amount of this diffusible protein moves towards the *sal*-negative cells, which activates vein-inducing signals that include genes such as *rho* (Sturtevant et al., 1997). Knockout of *sal* in clones of cells within a *sal*-expressing domain will create novel or missing boundaries of Sal+ against Sal− cells, and will result in ectopic or missing expression of *rho*, thus activating or inhibiting vein development.

In *B. anynana*, we observe Rho protein expression in the vein cells (Fig. 6E,F,K-M) and *bls* mRNA expression in the intervein cells (Fig. 6A-D). These expression domains are similar to those observed in *D. melanogaster* (Fristrom et al., 1994; Roch et al., 1998). This indicates that knocking out *sal* most likely results in ectopic or loss of Rho in the *B. anynana* wing, resulting in ectopic and disrupted vein phenotypes (Fig. 3S-X; Fig. S5M-X).

Inhibition of Dpp signaling results in venation defects likely due to reduced Sal expression

Inhibition of Dpp signaling using Dorsomorphin resulted in missing and ectopic veins, likely due to reduced Sal expression levels, along with overall reductions of wing size (Fig. 3D,G-I). Inhibition of Dpp in *Drosophila* has also resulted in similar phenotypes (Bosch et al., 2017). Dorsomorphin has been shown to block the phosphorylation of Mad (the signal transducer of Dpp) and to selectively inhibit BMP (Dpp) signaling (Yu et al., 2008). Injection of Dorsomorphin resulted in lower levels of *sal* gene expression in whole larval wings (Fig. 3I). Sal, as discussed above, is necessary for proper positioning of veins. Lower levels of Sal likely lead to missing and ectopic veins in Dorsomorphin-treated individuals (Fig. 3E-G). Knocking out *dpp*, using CRISPR-Cas9, produced similar ectopic as well as incomplete vein phenotypes at the Cu1 and Cu2 veins (Fig. 3H; Fig. S4H).

Wingless (Wg) signaling is not likely involved in the activation of the first and the third Sal domains in *Bicyclus*

To explore new ligands that might be involved in the activation of the first and third Sal domains, we studied Wg signaling. *wg* is expressed in the wing margin throughout the fifth instar larval wing development in butterflies (Fig. 5A,B; Fig. S7A-C; Martin and Reed, 2010, 2014). Arm, however, is homogeneously expressed during the early larval wing development (Fig. 5C,D). During later stages Arm becomes

Development (2020) 147, dev196394. doi:10.1242/dev.196394

expressed in the wing margin, along the veins, and in the eyespot centers (Fig. 5E,F; Connahs et al., 2019). The presence of Arm along the veins indicates that Wnt signaling might be involved in the maintenance of veins after they are set up. However, the inhibition of Wnt signaling during fourth instar development, using the drug iCRT3 (Lee et al., 2013), did not produce venation defects (Fig. 5G,H). Wnt inhibition reduced wing size and eyespot size (proportionately) and led to a few defects in the wing margin (Fig. 5G-I; Fig. S7E,F). Similar reduction in wing size without venation defects has also been observed in *D. melanogaster* (Couso et al., 1994). Reduction in both wing size and eyespot size, in a disproportionate degree relative to wing size, has been observed in *B. anynana* after a *wg*-RNAi knockdown was performed closer to the relevant stages of eyespot differentiation – at the end of the fifth instar and during the earliest stages of pupal development (Özsu et al., 2017). It is possible that the early injections of iCRT3, in fourth instar larvae, reduce wing size but have no subsequent effect on eyespot development, which occurs via a reaction-diffusion mechanism during the fifth instar (Connahs et al., 2019).

Loss of *sal*, *optix* and *dpp* expression domains likely led to venation simplification in *D. melanogaster*

Insect wing venation has simplified over the course of evolution, but it is unclear how exactly this simplification took place. Insect fossils from the Carboniferous period display many longitudinal veins in their wings compared with modern insects such as *D. melanogaster* or even *B. anynana* (Kukalova-Peck, 1978; Nel et al., 2007; Prokop and Ren, 2007). Many of the differences in venation remaining between *B. anynana* and *D. melanogaster* are due to the additional loss of veins in the posterior compartment in *D. melanogaster* (Fig. 7A-C). Sal expression domains and crispant phenotypes in *B. anynana* indicate that the third Sal expression domain, present in *B. anynana* but absent in *D. melanogaster*, is involved in the formation and arrangement of posterior veins Cu2 and A2 (Fig. 7F,K). In *D. melanogaster*, there is partial development of the Cu2+A1 (L6) vein and there are no A2 and A3 veins (Fig. 7B). The partial and missing veins in the posterior compartment of *D. melanogaster* are likely due to the reduction of the third and loss of the fourth Sal expression domains (Fig. 7H). It is also interesting to note that only one Optix domain is present in the upper anterior compartment in *D. melanogaster* (Fig. 7F), while in *B. anynana* we observe two domains, one in the upper anterior and one in the lower posterior compartment (Fig. 7K). The loss of the fourth Sal and second Optix domain was perhaps a consequence of the partial loss of the second *dpp* organizer (Fig. 7E), and the reduction of the third Sal domain in *D. melanogaster*. This reduced Sal domain was probably mediated by the delayed expression of a yet undiscovered organizer in this region (Y) that becomes activated only during the pupal stages in *D. melanogaster* (Fig. 7H).

Simplification of venation is also achieved via silencing of vein inducing or vein maintenance mechanisms

Vein number reduction via loss of *dpp*/*sal*/*optix* expression domains is one mechanism of vein reduction across evolution, but a different mechanism of vein reduction appears to take place downstream of the stable expression of these genes. For example, in *B. anynana*, we observe the development of veins at both boundaries of the second Sal domain (i.e. veins R2 and M3) (Fig. 7K), whereas in *D. melanogaster*, only cells abutting the anterior boundary of the homologous Sal expression domain activate the R2+3 (L2) vein (Sturtevant et al., 1997) (Fig. 7F). Vein activation proceeds via the activation of vein-inducing genes such as *knirps* and *rho*, which does not take place at the posterior boundary of Sal expression in *D. melanogaster* (Fig. 7F,H) (Sturtevant et al., 1997). In *B. anynana*, veins are also not being activated at the anterior boundary of the fourth Sal expression domain (in between the A2 and A3 veins) (Fig. 7K). It is still unclear why veins do not form at some boundaries of *sal* expression, but the paravein hypothesis proposes that loss of a vein-inducing program at these boundaries, resulted in venation simplification in modern insects such as *D. melanogaster* (Bier, 2000).

Further venation simplification might be happening via disruption of vein maintenance mechanisms, where vein induction is later followed by vein loss. In *D. melanogaster* the maintenance of vein identity involves the stable expression of Rho and the exclusion of Bls from vein cells throughout wing development (Blair, 2007; Fristrom et al., 1994). Disruptions to this mechanism, however, appear to be taking place at the A1 vein during *B. anynana* wing development (Fig. 6N-Q). The A1 vein is present during larval and early pupal wing development (Fig. 6N,O) but is absent in adults (Fig. 6P,Q). In *B. anynana*, *bls* is absent and Rho is present at the A1 vein in young larval wing discs (Fig. 6A,B,L; Fig. S7G; stage 0.5). However, as the wing grows, the expression of *bls* appears at the A1 vein, while Rho seems to disappear (Fig. 6C,D,M; Fig. S6H,I; stage 1.75). The detection of Rho using immunofluorescence is difficult at stage 1.75 (Fig. 6M), when *bls* was initially detected in the A1 vein, as tracheal tissues along the veins are auto-fluorescent. No staining was performed at later stages of development; however, early onset or the stable expression of *bls* at the A1 vein may result in the disappearance of this vein. It is unclear how the balance between Bls and presumably Rho expression is altered during development in the A1 veins of *B. anynana*, but such a mechanism likely contributes to the loss of that vein in adults and could contribute to vein loss, in general, across insects.

In conclusion, we have provided evidence for the presence of three main domains of gene expression in the early wings of butterflies – an anterior, middle and posterior domain – instead of two (anterior and posterior) domains, as observed in flies. We have found the presence of two *dpp* expression domains in butterfly wings. Furthermore, we have described and functionally characterized four domains of Sal expression and two domains of Optix expression in butterflies, the boundaries of which map to the development of multiple longitudinal veins in these insects. Two of the Sal domains and both the Optix domains straddle the two *dpp* expression domains, and may be activated by a *dpp* gradient, but Dpp or a different and yet undiscovered ligand (or ligands) is activating the two other Sal domains. The data presented in this study support a positional-information mechanism involved in venation patterning in Lepidoptera as is observed in Diptera. Moreover, the data provide support to the hypothesis of venation simplification in insects via loss of gene expression domains, silencing of vein-inducing boundaries (Biehs et al., 1998; Bier, 2000) and disruptions to vein maintenance programs (Blair, 2007). However, the mechanisms proposed in this article cannot explain every feature of insect venation. Insects with left-right wing differences in their longitudinal vein branching patterns, such as in the hemipteran *Orosanga japaonicus* (Yoshimoto and Kondo, 2012), and cross-vein patterns, such as in the hymenopteran *Athalia rosae* (Huang et al., 2018; Matsuda et al., 2013) and the odonate *Erythremis simplicicolis* (Hoffmann et al., 2018), most likely pattern their wings using both positional-information as well as reaction-diffusion mechanisms. The classic study by C. Waddington on the development of wild-type and mutant *D. melanogaster* wings (Waddington, 1940) probed many scientists to engage in the genetic control of wing development and venation in this

Development (2020) 147, dev196394. doi:10.1242/dev.196394

species. The genetic basis of wing venation evolution, however, has remained poorly explored. The present work will hopefully inspire others to engage in the study of additional insect species with variable venation patterns. Future comparative gene expression studies in these species, along with venation patterning modeling, should continue to illuminate the evolution and diversity of venation patterning mechanisms in insects.

MATERIALS AND METHODS

Animal husbandry

B. anynana butterflies were reared at 27°C in 12:12 day:night cycle. The larvae were fed young corn leaves and the adults were fed mashed bananas.

CRISPR-Cas9

Knockout of *sal*, *optix* and *dpp* was carried out using a protocol described previously (Banerjee and Monteiro, 2018). Briefly, for *sal* and *dpp* (see supplementary Materials and Methods for regions targeted by CRISPR), single guides were designed targeting exon 1 of *sal* and *dpp*; for *optix* (see Table S1), two guides were designed targeting exon 1 of *optix* (see Table S1). A total of 863 embryos for *sal*, 1973 embryos for *dpp* and 1509 embryos for *optix* were injected with each containing 300 ng/µl of guide (for *optix* both guides were used at the same time) and 300 ng/µl of Cas9 protein (NEB, M0641) mixed together in equal parts (total volume of 10 µl) with an added small amount of food dye (0.5 µl) (Tables S2-S4). The hatchlings were transferred into plastic cups and fed young corn leaves. After pupation, each individual was assigned a separate emergence compartment (a plastic cup with lid). Once eclosed, the adults were frozen at −20°C and imaged under a Leica DMS1000 (Olympus Corporation) microscope using LAS v4.9 (Leica Biosystems) software. Descaling of the adult wings for imaging was carried out using 100% Clorox solution (Patil and Magdum, 2017). Mutant individuals were tested for insertions or deletions via an *in vitro* endonuclease assay on the DNA isolated from the wings and then sequenced. For identification of indels, wings with CRISPR-Cas9 clones were dissected from frozen individuals. DNA was isolated using Omega E.Z.N.A. Tissue DNA Kit (D3396-01). After that, genes of interest were amplified using PCR and either sent for Illumina sequencing (for *opx* and *dpp*) or sequenced using Sanger sequencing (for *sal*).

In situ hybridization

Fifth instar larval wings were dissected based on a previously described protocol (Banerjee and Monteiro, 2020) in ice-cold PBS and transferred into 1× PBST supplemented with 4% formaldehyde for 30 min. After fixation, the wings were treated with 1.25 µl (20 mg/ml) proteinase K (NEB, P8107S) in 1 ml 1×PBST and then with 2 mg/ml glycine in 1×PBST. Afterwards, the wings were washed three times with 1×PBST, and the peripodial membrane was removed using fine forceps (Dumont, 11254-20) (in preparation for *in situ* hybridization). The wings were then gradually transferred into a pre-hybridization buffer (see Table S5 for composition) by increasing the concentration in 1×PBST and incubated in the pre-hybridization buffer for 1 h at 60°C. The wings were then incubated in hybridization buffer (see Table S5 for composition) supplemented with 100 ng/µl of probe at 60°C for 16-24 h. Subsequently, wings were washed five times with preheated pre-hybridization buffer at 60°C. The wings were then brought back to room temperature and transferred to 1× PBST by gradually increasing the concentration in the pre-hybridization buffer. They were later blocked in 1× PBST supplemented with 1% BSA for 1 h. After blocking, wings were incubated in 1:3000 anti-digoxygenin labeled probe diluted in block buffer. To localize the regions of gene expression, NBT/BCIP (Promega) in alkaline phosphatase buffer (see Table S5 for composition) was used. The wings were then washed, mounted in 60% glycerol and imaged under a Leica DMS1000 microscope using LAS v.4.9 (Leica Biosystems) software.

Immunostaining

Fifth instar larval wings were dissected based on a previously described protocol (Banerjee and Monteiro, 2020) in ice-cold PBS and immediately transferred into a fixation buffer supplemented with 4% formaldehyde (see Table S6 for composition) for 30 min. The wings were washed with 1×PBS and blocked for 1-2 days in block buffer (see Table S6 for composition) at 4°C. Wings were incubated in primary antibodies against En/Inv (1:20, mouse 4F11, a gift from Nipam Patel, Marine Biological Laboratory, Woods Hole, MA, USA; Patel et al., 1989), Sal (1:20,000, guinea-pig Sal GP66.1; Oliver et al., 2012), Arm (1:1000, rat Arm, see supplementary Materials and Methods), Opx (1:3000; rat Opx, a gift from Robert Reed, Cornell University, NY, USA; Martin et al., 2014), Rho (1:1000, rabbit Rho, see supplementary Materials and Methods) and Al (1:20, mouse DP311, a gift from Nipam Patel; Davis et al., 2005) at 4°C for 1 day, washed with wash buffer (see Table S6 for composition) and stained with secondary antibodies anti-mouse AF488 (Invitrogen, A28175), anti-rat AF488 (Invitrogen, A-11006), anti-rabbit AF488 (Invitrogen, A-11008) and anti-guinea pig AF555 (Invitrogen, A-21435) at a dilution of 1:500. The wings were then washed in wash buffer, mounted using an in-house mounting media (see Table S6 for composition) and imaged under an Olympus fv3000 confocal microscope.

Drug treatment and qPCR analysis

Fourth instar larvae were injected with 1 mM dorsomorphin (a BMP inhibitor) (Yu et al., 2008) and iCRT3 (a Wnt inhibitor) (Lee et al., 2013) in between the second and third thoracic legs on the left side of the body. DMSO (the solvent) was used as a control. A few of the individuals were dissected at late fifth instar larval wings based on the protocol described in Banerjee and Monteiro (2020) for qPCR analysis in a Bio-Rad qPCR thermocycler (three individuals in each biological replicate) and the rest were allowed to develop until adulthood. A total of four biological replicates of larval wing were tested for expression of *spalt* with three technical replicates. FK506 and UBQL40 were used as controls (Arun et al., 2015). Raw Cq data are provided in Table S7. Adult individuals were descaled in 100% Clorox solution (Patil and Magdum, 2017) and imaged under a Leica DMS1000 microscope.

Acknowledgements

We thank Jocelyn Wee for rearing *Pieris canidia*; Kenneth McKenna and Fred Nijhout for initial discussions on the paper; Robert Reed for anti-Optix antibody; Nipam Patel for the anti-Engrailed/Invected and anti-Aristaless antibodies; and Timothy Saunders, Christopher Winkler, Jocelyn Wee, Suriya Narayanan Murugesan, Sofia Sigal-Passeck and three anonymous reviewers for comments that improved the article. We also thank the DBS-CBIS confocal facility for access to the confocal microscopes.

Competing interests

The authors declare no competing or financial interests.

Author contributions

Conceptualization: T.D.B., A.M.; Methodology: T.D.B.; Software: T.D.B.; Validation: T.D.B., A.M.; Formal analysis: T.D.B., A.M.; Investigation: T.D.B.; Resources: A.M.; Data curation: T.D.B.; Writing - original draft: T.D.B.; Writing - review & editing: A.M.; Visualization: T.D.B.; Supervision: A.M.; Project administration: A.M.; Funding acquisition: A.M.

Funding

This work was supported by the Ministry of Education - Singapore (MOE2015-T2-2-159), by the National Research Foundation Singapore (NRF-NRFI05-2019-0006) and by the Department of Biological Sciences Lee Hiok Kwee fund (GL 710221). T.D.B. was supported by a Yale-NUS scholarship.

Supplementary information

Supplementary information available online at
https://dev.biologists.org/lookup/doi/10.1242/dev.196394.supplemental

Peer review history

The peer review history is available online at
https://dev.biologists.org/lookup/doi/10.1242/dev.196394.reviewer-comments.pdf

References

Abbasi, R. and Marcus, J. M. (2017). A new A-P compartment boundary and organizer in holometabolous insect wings. *Sci. Rep.* **7**, 16337. doi:10.1038/s41598-017-16553-5

Abouheif, E. and Wray, G. A. (2002). Evolution of the gene network underlying wing Polyphenism in ants. *Science* **297**, 249-252. doi:10.1126/science.1071468

Al Khatib, A., Siomava, N., Iannini, A., Posnien, N. and Casares, F. (2017). Specific expression and function of the Six3 optix in Drosophila serially homologous organs. *Biol. Open* **6**, 1155-1164. doi:10.1242/bio.023606
Arun, A., Baumlé, V., Amelot, G. and Nieberding, C. M. (2015). Selection and validation of reference genes for qRT-PCR expression analysis of candidate genes involved in olfactory communication in the butterfly bicyclus anynana. *PLoS ONE* **10**, e0120401. doi:10.1371/journal.pone.0120401
Banerjee, T. D. and Monteiro, A. (2018). CRISPR-Cas9 mediated genome editing in Bicyclus anynana butterflies. *Methods and Protoc.* **1**, 16. doi:10.3390/mps1020016
Banerjee, T. D. and Monteiro, A. (2020). Dissection of larval and pupal wings of Bicyclus anynana butterflies. *Methods Protoc.* **3**, 5. doi:10.3390/mps3010005
Banerjee, T. D., Ramos, D. and Monteiro, A. (2020). Expression of multiple engrailed family genes in eyespots of Bicyclus anynana butterflies does not implicate the duplication events in the evolution of this morphological novelty. *Front. Ecol. Evol.* **8**, 493. doi:10.3389/fevo.2020.00227
Barrio, R. and De Celis, J. F. (2004). Regulation of spalt expression in the Drosophila wing blade in response to the Decapentaplegic signaling pathway. *Proc. Natl. Acad. Sci. USA* **101**, 6021-6026. doi:10.1073/pnas.0401590101
Biehs, B., Sturtevant, M. A. and Bier, E. (1998). Boundaries in the Drosophila wing imaginal disc organize vein-specific genetic programs. *Development* **125**, 4245-4257.
Bier, E. (2000). Drawing lines in the Drosophila wing: initiation of wing vein development. *Curr. Opin. Genet. Dev.* **10**, 393-398. doi:10.1016/S0959-437X(00)00102-7
Blair, S. S. (1992). Engrailed expression in the anterior lineage compartment of the developing wing blade of Drosophila. *Development* **115**, 21-33.
Blair, S. S. (2007). Wing vein patterning in Drosophila and the analysis of intercellular signaling. *Annu. Rev. Cell Dev. Biol.* **23**, 293-319. doi:10.1146/annurev.cellbio.23.090506.123606
Bosch, P. S., Ziukaite, R., Alexandre, C., Basler, K. and Vincent, J. P. (2017). Dpp controls growth and patterning in Drosophila wing precursors through distinct modes of action. *eLife* **6**, e22546. doi:10.7554/eLife.22546
Carroll, S. B., Gates, J., Keys, D. N., Paddock, S. W., Panganiban, G. E., Selegue, J. E. and Williams, J. A. (1994). Pattern formation and eyespot determination in butterfly wings. *Science* **265**, 109-114. doi:10.1126/science.7912449
Cheng, Y., Brunner, A. L., Kremer, S., DeVido, S. K., Stefaniuk, C. M. and Kassis, J. A. (2014). Co-regulation of invected and engrailed by a complex array of regulatory sequences in Drosophila. *Dev. Biol.* **395**, 131-143. doi:10.1016/j.ydbio.2014.08.021
Chintapalli, R. T. V. and Hillyer, J. F. (2016). Hemolymph circulation in insect flight appendages: physiology of the wing heart and circulatory flow in the wings of the mosquito *Anopheles gambiae*. *J. Exp. Biol.* **219**, 3945-3951. doi:10.1242/jeb.148254
Combes, S. A. (2003). Flexural stiffness in insect wings I. Scaling and the influence of wing venation. *J. Exp. Biol.* **206**, 2979-2987. doi:10.1242/jeb.00523
Comstock, J. H. and Needham, J. G. (1898). The wings of insects. *Am. Soc. Nat.* **32**, 43-48. doi:10.1086/276766
Connahs, H., Tlili, S., van Creij, J., Loo, T. Y. J., Banerjee, T. D., Saunders, T. E. and Monteiro, A. (2019). Activation of butterfly eyespots by distal-less is consistent with a reaction-diffusion process. *Development* **146**, dev169367. doi:10.1242/dev.169367
Cook, O., Biehs, B. and Bier, E. (2004). brinker and optomotor-blind act coordinately to initiate development of the L5 wing vein primordium in Drosophila. *Development* **131**, 2113-2124. doi:10.1242/dev.01100
Couso, J. P., Bishop, S. A. and Martinez Arias, A. (1994). The wingless signalling pathway and the patterning of the wing margin in Drosophila. *Development* **120**, 621-636.
Davis, G. K., D'Alessio, J. A. and Patel, N. H. (2005). Pax3/7 genes reveal conservation and divergence in the arthropod segmentation hierarchy. *Dev. Biol.* **285**, 169-184. doi:10.1016/j.ydbio.2005.06.014
De Celis, J. F. (2003). Pattern formation in the Drosophila wing: the development of the veins. *BioEssays* **25**, 443-451. doi:10.1002/bies.10258
De Celis, J. F. and Diaz-Benjumea, F. J. (2003). Developmental basis for vein pattern variations in insect wings. *Int. J. Dev. Biol.* **47**, 653-663.
Dion, E., Monteiro, A. and Yew, J. Y. (2016). Phenotypic plasticity in sex pheromone production in Bicyclus anynana butterflies. *Sci. Rep.* **6**, 39002. doi:10.1038/srep39002
Foronda, D., Pérez-Garijo, A. and Martín, F. A. (2009). Dpp of posterior origin patterns the proximal region of the wing. *Mech. Dev.* **126**, 99-106. doi:10.1016/j.mod.2008.12.002
Fristrom, D., Gotwals, P., Eaton, S., Kornberg, T. B., Sturtevant, M. and Fristrom, J. W. (1994). Blistered: a gene required for vein/intervein formation in wings of Drosophila. **2671**, 2661-2671.
Gantz, V. M. (2015). The mutagenic chain reaction: from Evo-Devo to active genetics. Calif. Digit. Libr. (University California, San Diego).
Garcia-bellido, A. and De Celis, J. F. (1992). Developmental genetics of the venation pattern: origin of wing veins. *Annu. Rev. Genet.* **1940**, 28.
Grieder, N. C., Morata, G., Affolter, M. and Gehring, W. J. (2009). Spalt major controls the development of the notum and of wing hinge primordia of the Drosophila melanogaster wing imaginal disc. *Dev. Biol.* **329**, 315-326. doi:10.1016/j.ydbio.2009.03.006
Guichard, A., Biehs, B., Sturtevant, M. A., Wickline, L., Chacko, J., Howard, K. and Bier, E. (1999). rhomboid and star interact synergistically to promote EGFR/MAPK signaling during Drosophila wing vein development. *Development* **126**, 2663-2676.
Guillén, I., Mullor, J. L., Capdevila, J., Sánchez-Herrero, E., Morata, G. and Guerrero, I. (1995). The function of *engrailed* and the specification of *Drosophila* wing pattern. *Development* **121**, 3447-3456.
Hoffmann, J., Donoughe, S., Li, K., Salcedo, M. K. and Rycroft, C. H. (2018). A simple developmental model recapitulates complex insect wing venation patterns. *Proc. Natl. Acad. Sci. USA* **115**, 9905-9910. doi:10.1073/pnas.1721248115
Huang, Y., Hatakeyama, M. and Shimmi, O. (2018). Wing vein development in the sawfly Athalia rosae is regulated by spatial transcription of Dpp/BMP signaling components. *Arthropod Struct. Dev.* **47**, 408-415. doi:10.1016/j.asd.2018.03.003
Ingham, P. W. and Fietz, M. J. (1995). Quantitative effects of hedgehog and decapentaplegic activity on the patterning of the Drosophila wing. *Curr. Biol.* **5**, 432-440. doi:10.1016/S0960-9822(95)00084-4
Jiggins, C. D., Wallbank, R. W. R. and Hanly, J. J. (2017). Waiting in the wings: what can we learn about gene co-option from the diversification of butterfly wing patterns? *Philos. Trans. R. Soc. B Biol. Sci.* **372**, 20150485. doi:10.1098/rstb.2015.0485
Kaba, D., Berté, D., Ta, B. T. D., Tellería, J., Solano, P. and Dujardin, J.-P. (2017). The wing venation patterns to identify single tsetse flies. *Infect. Genet. Evol.* **47**, 132-139. doi:10.1016/j.meegid.2016.10.008
Keys, D. N., Lewis, D. L., Selegue, J. E., Pearson, B. J., Goodrich, L. V., Johnson, R. L., Gates, J., Scott, M. P. and Carroll, S. B. (1999). Recruitment of a hedgehog regulatory circuit in butterfly eyespot evolution. *Science* **283**, 532-534. doi:10.1126/science.283.5401.532
Koch, P. B. and Nijhout, H. F. (2002). The role of wing veins in colour pattern development in the butterfly Papilio xuthus (Lepidoptera: Papilionidae). *Eur. J. Entomol.* **99**, 67-72. doi:10.14411/eje.2002.012
Kosman, D., Small, S. and Reinitz, J. (1998). Rapid preparation of a panel of polyclonal antibodies to Drosophila segmentation proteins. *Dev. Genes Evol.* **208**, 290-294. doi:10.1007/s004270050184
Kukalova-Peck, J. (1978). Origin and evolution of insect wings and their relation to metamorphosis, as documented by the fossil record. *J. Morphol.* **156**, 53-125. doi:10.1002/jmor.1051560104
Lawrence, P. A., Casal, J., de Celis, J. F. and Morata, G. (2017). A refutation to 'A new A-P compartment boundary and organizer in holometabolous insect wings'. *Sci. Rep.* **7**, 7049. doi:10.1038/s41598-019-42668-y
Lee, E., Madar, A., David, G., Garabedian, M. J., DasGupta, R. and Logan, S. K. (2013). Inhibition of androgen receptor and β-catenin activity in prostate cancer. *Proc. Natl. Acad. Sci. USA* **110**, 15710-15715. doi:10.1073/pnas.1218168110
Lunde, K., Biehs, B., Nauber, U. and Bier, E. (1998). The knirps and knirps-related genes organize development of the second wing vein in Drosophila. *Development* **125**, 4145-4154.
Martin, A. and Reed, R. D. (2010). wingless and aristaless2 define a developmental ground plan for moth and butterfly wing pattern evolution. *Mol. Biol. Evol.* **27**, 2864-2878. doi:10.1093/molbev/msq173
Martin, A. and Reed, R. D. (2014). Wnt signaling underlies evolution and development of the butterfly wing pattern symmetry systems. *Dev. Biol.* **395**, 367-378. doi:10.1016/j.ydbio.2014.08.031
Martin, A., McCulloch, K. J., Patel, N. H., Briscoe, A. D., Gilbert, L. E. and Reed, R. D. (2014). Multiple recent co-options of optix associated with novel traits in adaptive butterfly wing radiations. *Evodevo* **5**, 7. doi:10.1186/2041-9139-5-7
Martín, M., Ostalé, C. M. and De Celis, J. F. (2017). Patterning of the drosophila L2 vein is driven by regulatory interactions between region-specific transcription factors expressed in response to Dpp signalling. *Development* **144**, 3168-3176. doi:10.1242/dev.143461
Matsuda, S. and Affolter, M. (2017). Dpp from the anterior stripe of cells is crucial for the growth of the Drosophila wing disc. *eLife* **6**, e22319. doi:10.7554/eLife.22319
Matsuda, S., Yoshiyama, N., Künnapuu-Vulli, J., Hatakeyama, M. and Shimmi, O. (2013). Dpp/BMP transport mechanism is required for wing venation in the sawfly Athalia rosae. *Insect Biochem. Mol. Biol.* **43**, 466-473. doi:10.1016/j.ibmb.2013.02.008
Monteiro, A., Glaser, G., Stockslager, S., Glansdorp, N. and Ramos, D. (2006). Comparative insights into questions of lepidopteran wing pattern homology. *BMC Dev. Biol.* **6**, 52. doi:10.1186/1471-213X-6-52
Nel, A., Roques, P., Nel, P., Prokop, J. and Steyer, J. S. (2007). The earliest holometabolous insect from the Carboniferous: a "crucial" innovation with delayed success (Insecta Protomeropina Protomeropidae). *Ann. de la Soc. Entomol. de France (N.S.).* **43**, 349-355. doi:10.1080/00379271.2007.10697531
Nowell, R. W., Elsworth, B., Oostra, V., Zwaan, B. J., Wheat, C. W., Saastamoinen, M., Saccheri, I. J., van't Hof, A. E., Wasik, B. R., Connahs, H. et al. (2017). A high-coverage draft genome of the mycalesine butterfly Bicyclus anynana. *Gigascience* **6**, 1-7. doi:10.1093/gigascience/gix035

Oliver, J. C., Tong, X. L., Gall, L. F., Piel, W. H. and Monteiro, A. (2012). A single origin for nymphalid butterfly eyespots followed by widespread loss of associated gene expression. *PLoS Genet.* **8**, e1002893-355. doi:10.1371/journal.pgen.1002893

Organista, M. F. and De Celis, J. F. (2013). The Spalt transcription factors regulate cell proliferation, survival and epithelial integrity downstream of the Decapentaplegic signalling pathway. *Biol. Open* **2**, 37-48. doi:10.1242/bio.20123038

Özsu, N., Chan, Q. Y., Chen, B., Gupta, M. D. and Monteiro, A. (2017). Wingless is a positive regulator of eyespot color patterns in Bicyclus anynana butterflies. *Dev. Biol.* **429**, 177-185. doi:10.1016/j.ydbio.2017.06.030

Patel, N. H., Martin-Blanco, E., Coleman, K. G., Poole, S. J., Ellis, M. C., Kornberg, T. B. and Goodman, C. S. (1989). Expression of engrailed proteins in arthropods, annelids, and chordates. *Cell* **58**, 955-968. doi:10.1016/0092-8674(89)90947-1

Patil, S. and Magdum, S. (2017). Insight into wing venation in butterflies belonging to families Papilionidae, Nymphalidae and Pieridae from Dang Dist Gujarat, India. *J. Entomol. Zool. Stud.* **5**, 1596-1607.

Prokop, J. and Ren, D. (2007). New significant fossil insects from the upper Carboniferous of Ningxia in northern China (Palaeodictyoptera, Archaeorthoptera). *Eur. J. Entomol.* **104**, 267-275. doi:10.14411/eje.2007.041

Reed, R. D., Chen, P.-H. and Frederik Nijhout, H. (2007). Cryptic variation in butterfly eyespot development: The importance of sample size in gene expression studies. *Evol. Dev.* **9**, 2-9. doi:10.1111/j.1525-142X.2006.00133.x

Reed, R. D., Papa, R., Martin, A., Hines, H. M., Counterman, B. A., Pardo-Diaz, C., Jiggins, C. D., Chamberlain, N. L., Kronforst, M. R., Chen, R. et al. (2011). optix drives the repeated convergent evolution of butterfly wing pattern mimicry. *Science* **333**, 1137-1141. doi:10.1126/science.1208227

Roch, F., Baonza, F., Martín-Blanco, E., García-Bellido, A., Baonza, A., Martin-Blanco, E. and Garcia-Bellido, A. (1998). Genetic interactions and cell behaviour in blistered mutants during proliferation and differentiationof the Drosophila wing. *Development* **125**, 1823-1832.

Saenko, S. V., Marialva, M. S. P. and Beldade, P. (2011). Involvement of the conserved Hox gene Antennapedia in the development and evolution of a novel trait. *Evodevo* **2**, 9. doi:10.1186/2041-9139-2-9

Schachat, S. R. and Brown, R. L. (2015). Color pattern on the forewing of Micropterix (Lepidoptera: Micropterigidae): insights into the evolution of wing pattern and wing venation in moths. *PLoS ONE* **10**, e0139972. doi:10.1371/journal.pone.0139972

Simcox, A. A., Grumbling, G., Schnepp, B., Bennington-Mathias, C., Hersperger, E. and Shearn, A. (1996). Molecular, phenotypic, and expression analysis of vein, a gene required for growth of the Drosophila wing disc. *Dev. Biol.* **177**, 475-489. doi:10.1006/dbio.1996.0179

Stark, J., Bonacum, J., Remsen, J. and DeSalle, R. (1999). The evolution and development of dipteran wing veins: a systematic approach. *Annu. Rev. Entomol.* **44**, 97-129. doi:10.1146/annurev.ento.44.1.97

Stoehr, A. M., Walker, J. F. and Monteiro, A. (2013). Spalt expression and the development of melanic color patterns in pierid butterflies. *Evodevo* **4**, 6. doi:10.1186/2041-9139-4-6

Strigini, M. and Cohen, S. M. (1999). Formation of morphogen gradients in the Drosophila wing. *Semin Cell Dev. Biol.* **10**, 335-344. doi:10.1006/scdb.1999.0293

Sturtevant, M. A., Biehs, B., Marin, E. and Bier, E. (1997). The spalt gene links the A/P compartment boundary to a linear adult structure in the Drosophila wing. *Development* **124**, 21-32.

Sun, P., Mhatre, N., Mason, A. C. and Yack, J. E. (2018). In that vein: inflated wing veins contribute to butterfly hearing. *Biol. Lett.* **14**, 20180496. doi:10.1098/rsbl.2018.0496

Szuperak, M., Salah, S., Meyer, E. J., Nagarajan, U., Ikmi, A. and Gibson, M. C. (2011). Feedback regulation of Drosophila BMP signaling by the novel extracellular protein Larval Translucida. *Development* **138**, 715-724. doi:10.1242/dev.059477

Tabata, T., Eaton, S. and Kornberg, T. B. (1992). The Drosophila hedgehog gene is expressed specifically in posterior compartment cells and is a target of engrailed regulation. *Genes Dev.* **6**, 2635-2645. doi:10.1101/gad.6.12b.2635

Tanimoto, H., Itoh, S., Ten Dijke, P. and Tabata, T. (2000). Hedgehog creates a gradient of DPP activity in Drosophila wing imaginal discs. *Mol. Cell* **5**, 59-71. doi:10.1016/S1097-2765(00)80403-7

Tomoyasu, Y., Wheeler, S. R. and Denell, R. E. (2005). Ultrabithorax is required for membranous wing identity in the beetle Tribolium castaneum. *Nature* **433**, 643-647. doi:10.1038/nature03272

Waddington, C. H. (1940). The genetic control of wing development in Drosophila. *J. Genet.* **41**, 75-113. doi:10.1007/BF02982977

Wang, D., Li, J., Liu, S., Zhou, H., Zhang, L., Shi, W. and Shen, J. (2017). spalt is functionally conserved in Locusta and Drosophila to promote wing growth. *Sci. Rep.* **7**, 44393. doi:10.1038/srep44393

Westerman, E. L., VanKuren, N. W., Massardo, D., Tenger-Trolander, A., Zhang, W., Hill, R. I., Perry, M., Bayala, E., Barr, K., Chamberlain, N. et al. (2018). Aristaless controls butterfly wing color variation used in mimicry and mate choice. *Curr. Biol.* **28**, 3469-3474.e4. doi:10.1016/j.cub.2018.08.051

Yoshimoto, E. and Kondo, S. (2012). Wing vein patterns of the Hemiptera insect Orosanga japonicus differ among individuals. *Interface Focus* **2**, 451-456. doi:10.1098/rsfs.2011.0112

Yu, P. B., Hong, C. C., Sachidanandan, C., Babitt, J. L., Deng, D. Y., Hoyng, S. A., Lin, H. Y., Bloch, K. D. and Peterson, R. T. (2008). Dorsomorphin inhibits BMP signals required for embryogenesis and iron metabolism. *Nat. Chem. Biol.* **4**, 33-41. doi:10.1038/nchembio.2007.54

Zhang, L., Martin, A., Perry, M. W., van der Burg, K. R. L., Matsuoka, Y., Monteiro, A. and Reed, R. D. (2017). Genetic basis of melanin pigmentation in butterfly wings. *Genetics* **205**, 1537-1550. doi:10.1534/genetics.116.196451

Supplementary Materials

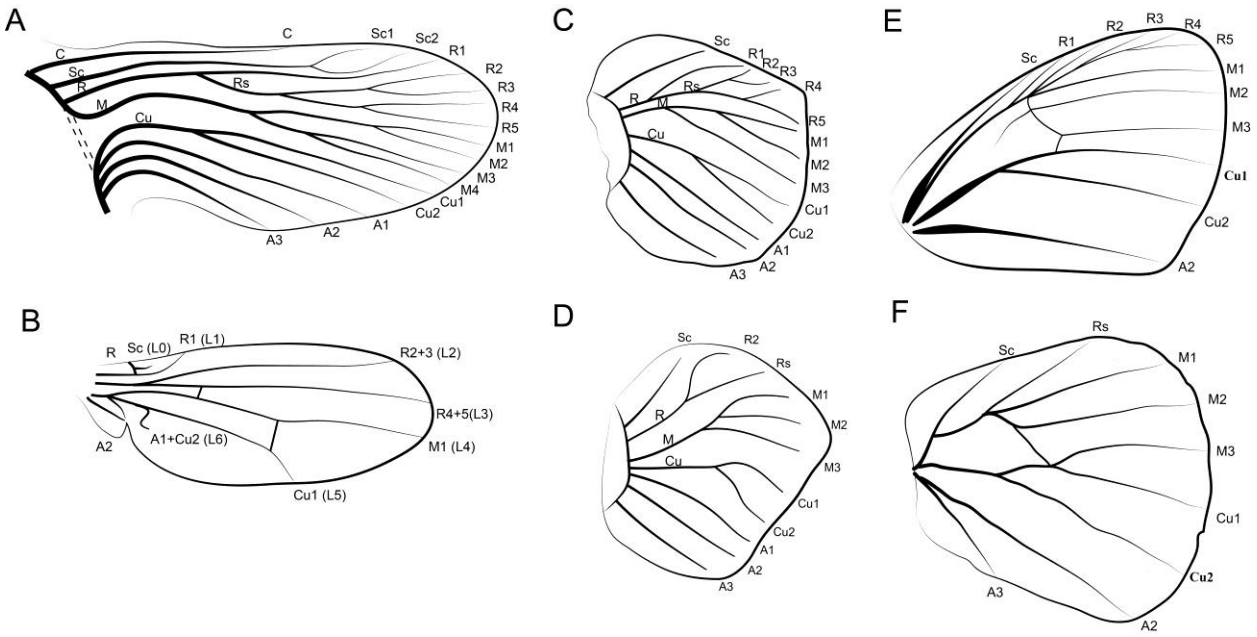

Figure S1. Venation patterns in insects. (A) Comstock-Needham hypothetic venation of primitive insects (redrawn from (Comstock and Needham, 1898)), **(B)** Wing venation of *Drosophila melanogaster* (redrawn from (Blair, 2007)), **(C)** Larval forewing venation and **(D)** hindwing venation of *Bicyclus anynana* butterflies. Larval wings of *B. anynana* were drawn based on methylene blue staining's (**Fig. S5**). **(E)** Adult forewing and **(F)** hindwing venation of *B. anynana*.

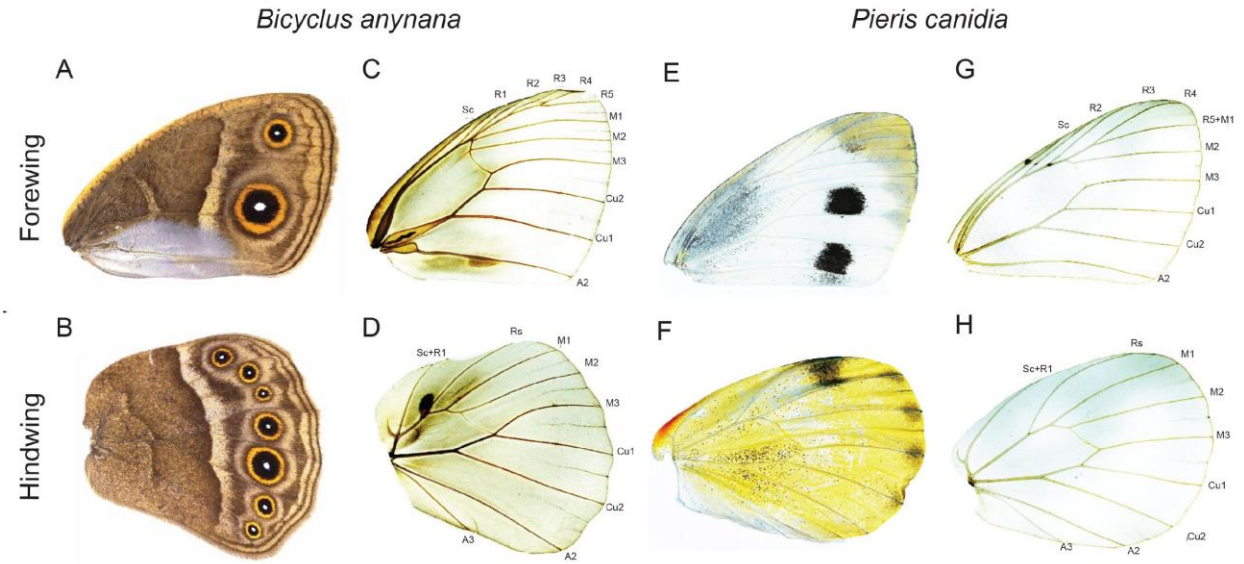

Figure S2. Venation pattern in adult butterflies. (A and C) *Bicyclus anynana* forewing, **(B and D)** and hindwing. **(E and G)** *Pieris canidia* forewing, **(F and H)** and hindwing. **(A, B, E and F)** Adult wings with scales. **(C, D, G, and H)** Adult wings with scales removed.

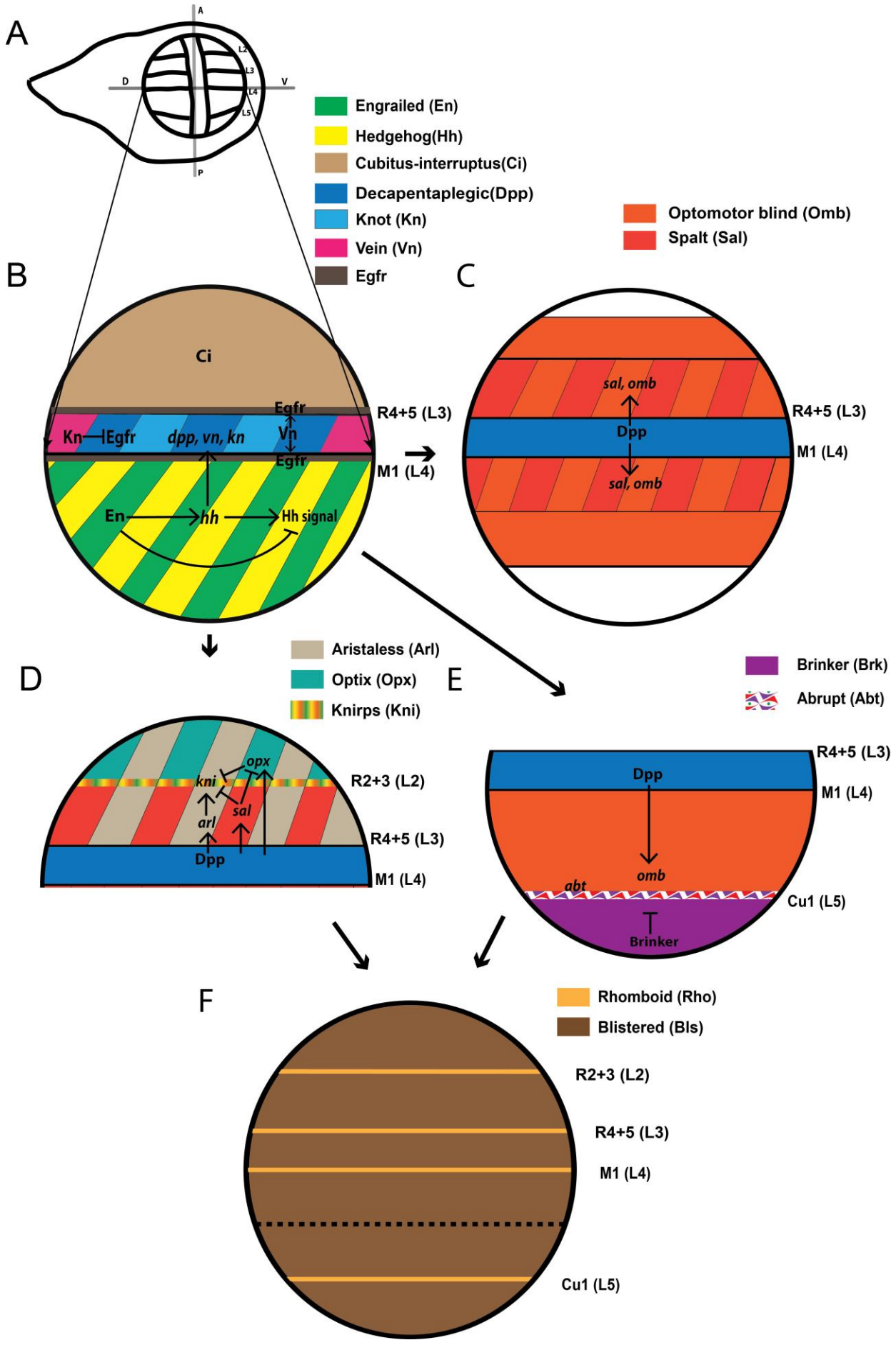

Figure S3. Molecular mechanism involved in venation patterning in *Drosophila melanogaster*. (A) Larval wing disc of *D. melanogaster*. During the larval stage, the wing is divided into two populations of immiscible cells belonging to the Anterior (A) and Posterior (P) compartments. The boundary where these two-populations meets is referred to as the Anterior-Posterior (A-P) boundary (marked by the gray line). **(B)** Venation patterning is initiated by the transcription factors En and Inv in the posterior compartment that activate expression of *hh* while suppressing Hh signaling. Hh is a short-range diffusible morphogen. A small amount of Hh diffuses into the anterior compartment where the presence of Ci activates the BMP ligand *dpp*. Hh also activates the genes *vein* and *knot* overlapping the expression of *dpp*. Knot inhibits Egfr signaling at the R4+5 (L3) and M1 (L4) intervein cells. The veins R4+5 (L3) and M1 (L4) form at the anterior and posterior boundary of the *dpp* and *vein* expression domain due to activation of Egfr signaling via Vein protein. **(C)** Dpp protein then acts as a long-range morphogen activating both *spalt* (*sal*) and *optomotor-blind* (*omb*) at high concentrations, and only *omb* when the concentration falls below the *sal*-inducing threshold. (**D**) The vein R2+3 (L2) forms by the interaction of Al, Opx and Sal. Dpp activates all three transcription factors at different concentration thresholds. Al activates the R2+3 (L2) vein specific gene *knirps*, Sal represses *opx*, and Opx and Sal suppresses *knirps*. (**E**) The vein Cu1 (L5) forms at the boundary of Omb and Brinker where the Cu1 (L5) specific gene *abrupt* is expressed. (**F**) The final step of venation patterning involves expression of Rho in the vein cells and Bls in the intervein cells.

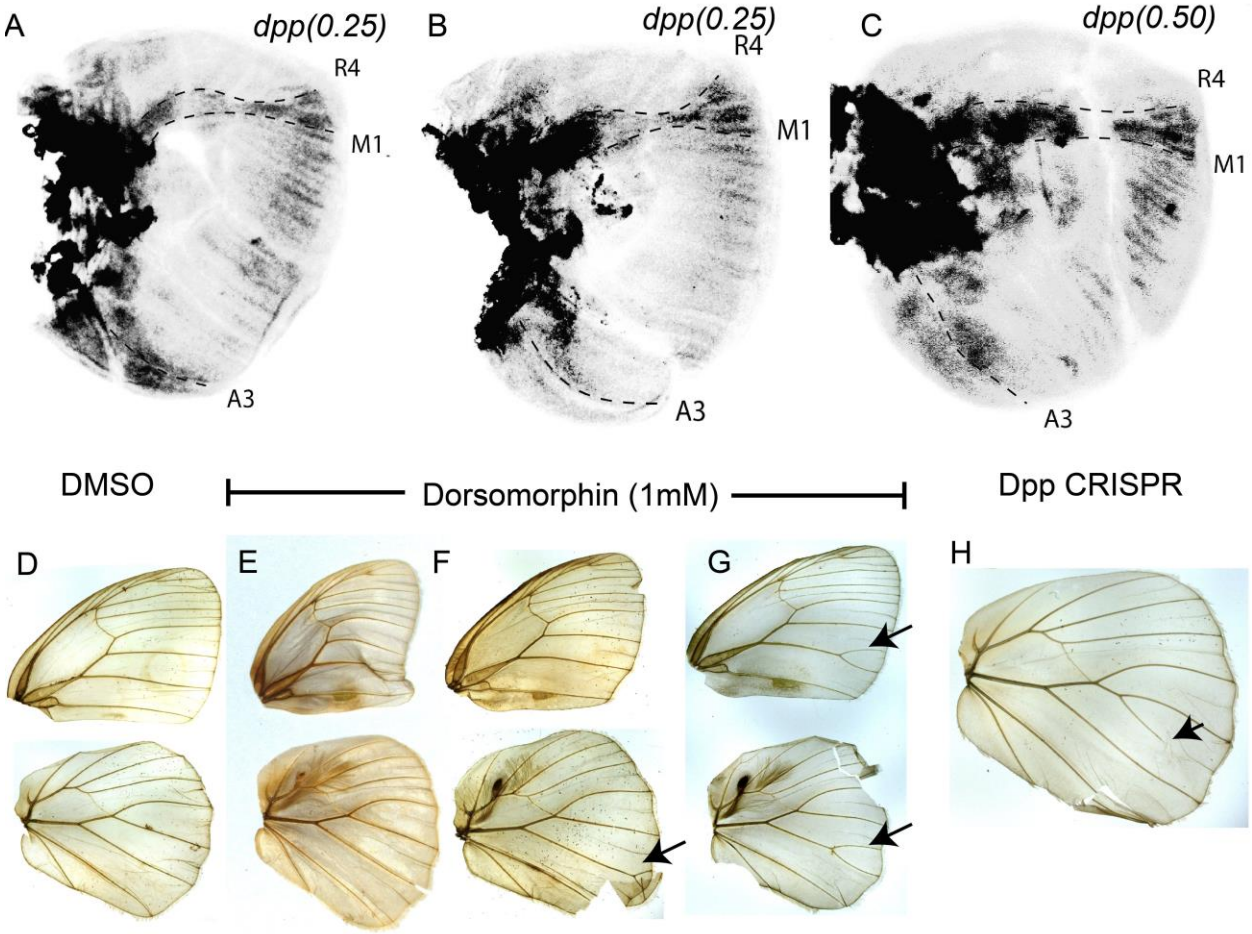

Figure S4. Expression of *decapentaplegic* (*dpp*) and the effect of Dorsomorphin and Dpp CRISPR on the wings of *Bicyclus anynana*. (A-C) *dpp* is expressed in two domains in the larval wings. (**D**) Adult descaled Wings of a control individual injected with DMSO. (**E-G**) Dorsomorphin affects the wing size and venation (black arrow). (**H**) Dpp CRISPR individual with ectopic and missing vein (black arrow).

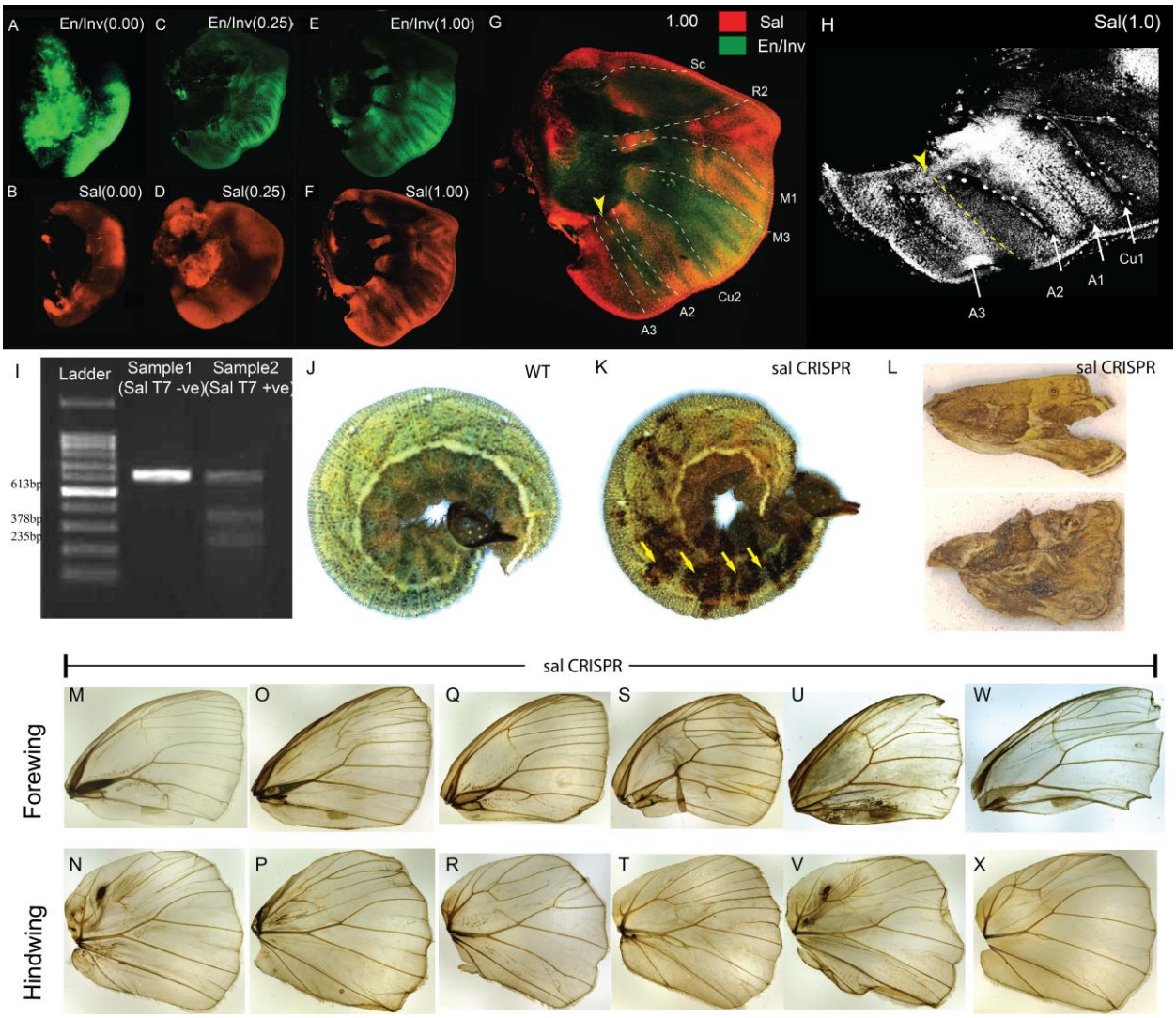

Figure S5. Expression of Spalt (Sal) and Engrailed /Invected (En/Inv); and function of *sal* in *Bicyclus anynana*. (**A, C, and E**) En/Inv staining at different stages of larval wing growth. **(B, D, and F**) Sal staining at different stages of wing growth. (**G**) Merged channels of Sal and En/Inv. **(H)** Closeup of Sal expression showing the anterior boundary of the fourth Sal domain (yellow arrowhead and dotted yellow line). (**I**) T7 endonuclease assay on *sal* guide and Cas9 injected individuals. Sample 2 with T7 endonuclease added shows two shorter DNA bands indicating cleavage of the PCR product. **(J)** A WT fifth instar larva. (**K**) Pigmentation defects on sal CRISPR larva. Spalt has been implicated to be involved in the development of black pigment on the eyespots of *B. anynana* butterflies. (**L**) Severe adult wing patterning defects in some individuals were observed. **(M-X)** Venation defects in *B. anynana* descaled adult forewings and hindwings.

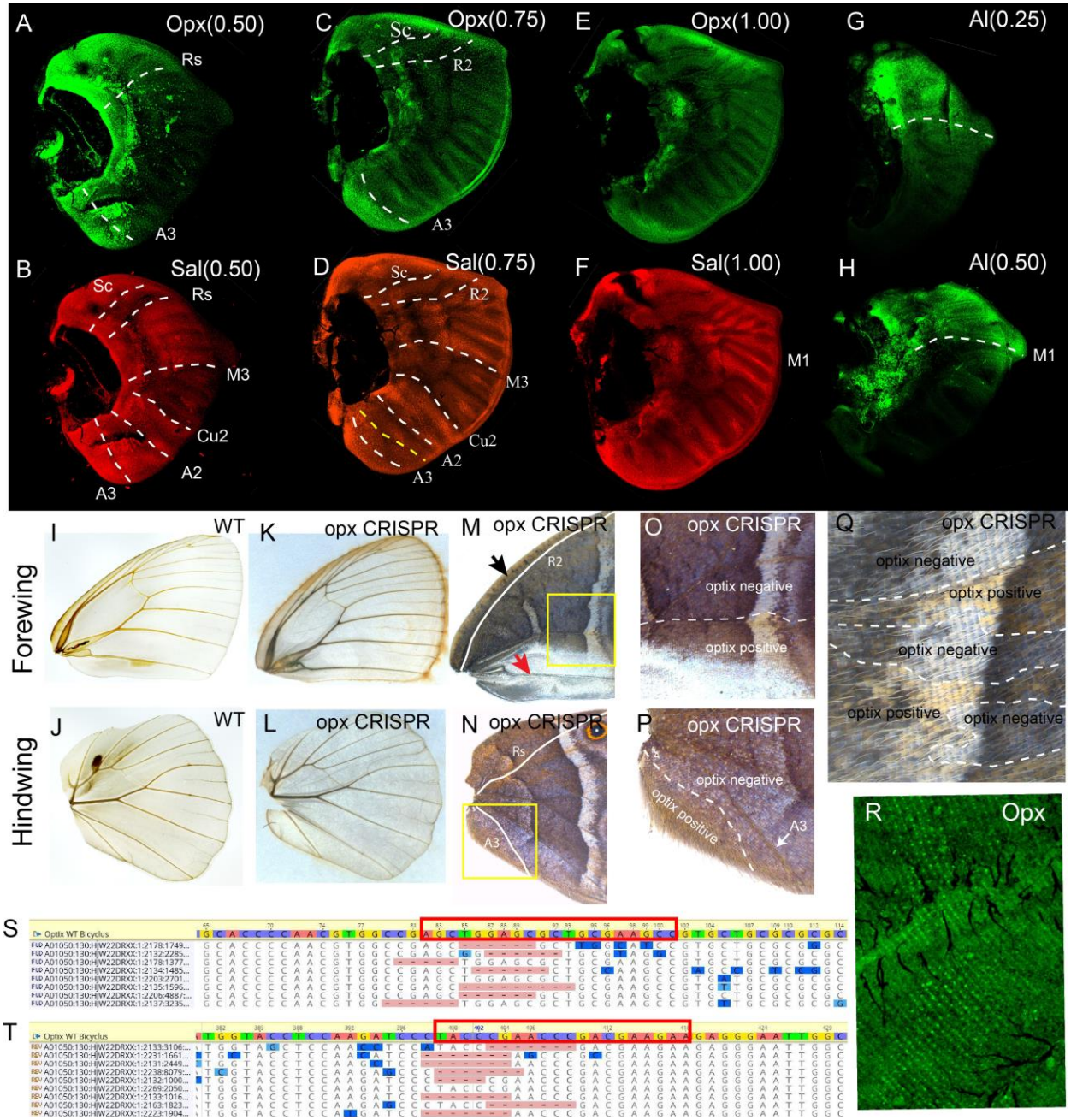

Figure S6. Expression of Optix (Opx) and Aristaless (Al); and function of *opx* in *Bicyclus anynana*. Opx expression at different stages of larval wing growth in the (**A, C and E)**. Sal expression at different stages of larval wing growth **(B, D, and F)**. (**G and H**) Al expression at different stages of larval wing growth. WT descaled adult (**I**) forewing and (**J**) hindwing. Optix CRISPR (**K**) forewing and (**L**) hindwing. No defects in venation are observed. (**M-Q**) Optix CRISPR individuals with loss of scales with ommochrome (orange) pigment. (**R**) Optix expression in the pupal wings. (**S and T**) Deletions in the regions targeted for *optix* CRISPR (red boxes). Black arrow: orange scales in the anterior margin of the forewing overlap the anterior expression of Optix in the larval wing disc. Red arrow: silver scales in the posterior region of the forewing overlap the posterior expression of Optix in the larval wing disc.

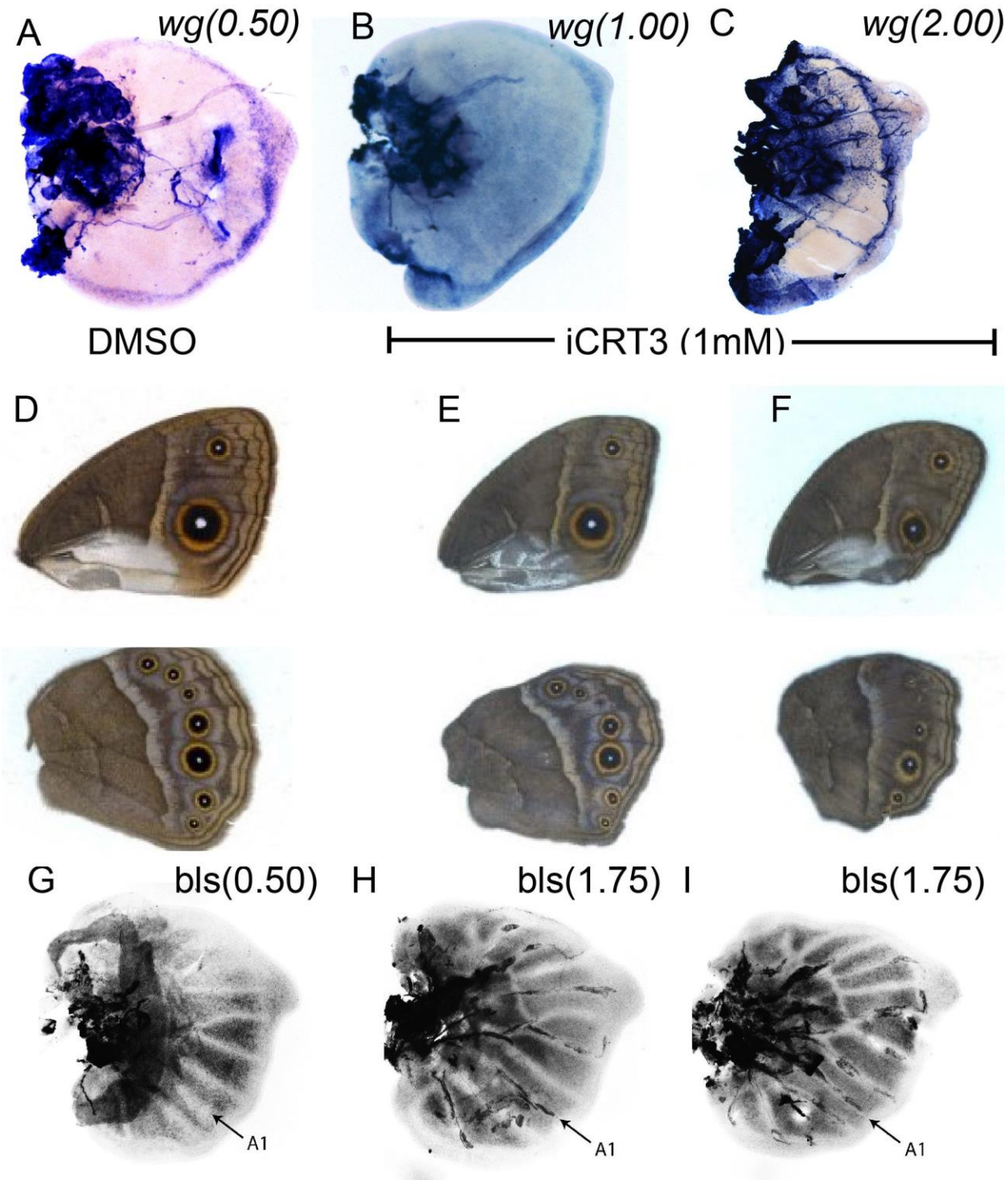

Figure S7. **Expression of *wingless* (*wg*) and *blistered* (*bls*); and the effect of iCRT3 on the wings of *Bicyclus anynana*.** (**A-C**) Expression of *wg* in the larval wing margin. (**D**) Adult wings of a control individual injected with DMSO. (**E and F**) iCRT3 injections reduce the adult wing size relative to DMSO injections. (**G-I**) Expression of *bls* in larval wings. *bls* is absent at the A1 vein at an early stage (0.50). However, during later stages (1.75) *bls* has a stronger expression at the A1 vein.

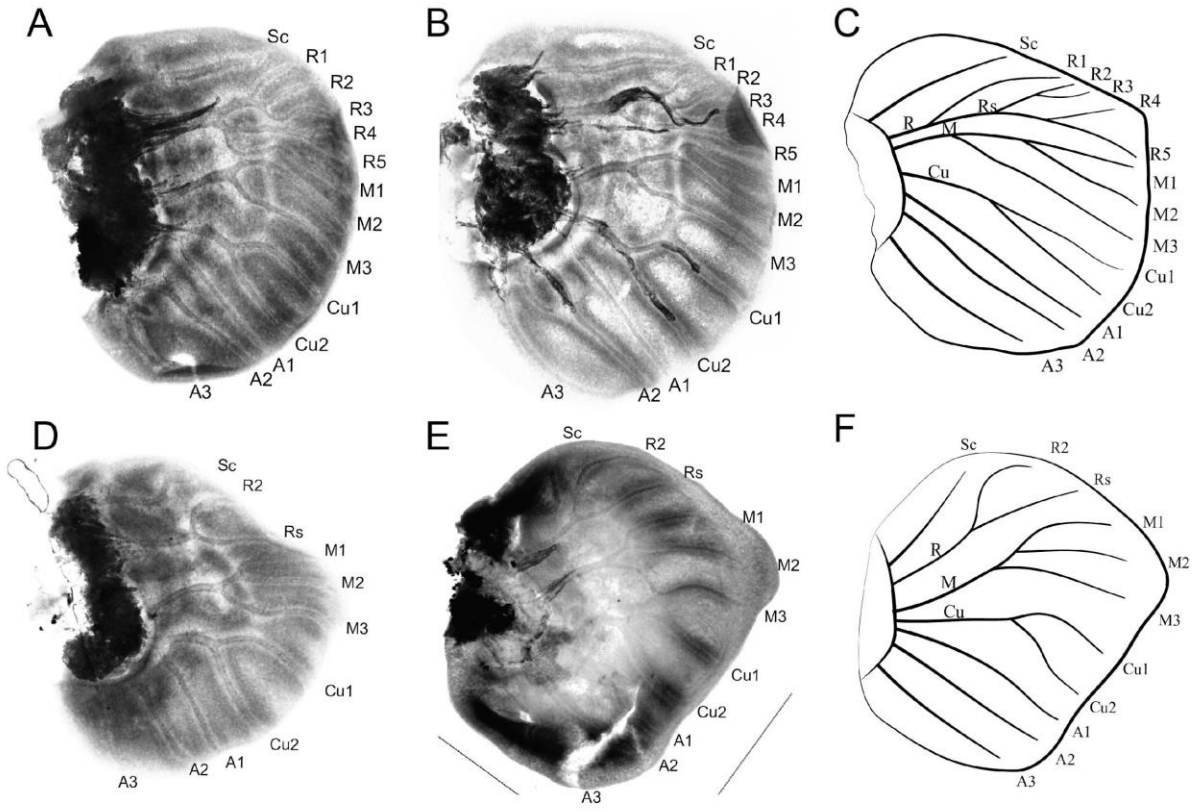

Figure S8. Methylene blue staining of *Bicyclus anynana* larval wings. (A and B) Forewing stained with methylene blue; **(D and E)** Hindwing stained with methylene blue; Illustration of (**C**) forewing and (**F**) hindwing venation.

Table S1. Primer table

No.	Primer Name	Sequence	Description
1.	Dpp_insitu_F	GTTCTTCAACGTAAGCGGCG	Forward primer to amplify *dpp* for in-situ hybridization
2.	Dpp_insitu_R	CCACAGCCTACCACCATCAT	Reverse primer to amplify *dpp* for in-situ hybridization
3.	En_insitu_F	TTGAAGACCGTTGCAGTCC	Forward primer to amplify *en* for in-situ hybridization
4.	En_insitu_R	TAGATTGCTGTTCCCGCTTT	Reverse primer to amplify *en* for in-situ hybridization
5.	Inv_insitu_F	GGACCAAAGTGACGAAGAGC	Forward primer to amplify *inv* for in-situ hybridization
6.	Inv_insitu_R	TCCGGCACTCTAGCCTCTAC	Reverse primer to amplify *inv* for in-situ hybridization
7.	Bls_insitu_F	CTGACCGGCACCCAAGTGAT	Forward primer to amplify *bls* for in-situ hybridization
8.	Bls_insitu_R	CGTTGCGGGTGGTGAGACAT	Reverse primer to amplify *bls* for in-situ hybridization
9.	Sal_CRISPR_Seq_F	GCATCGACAAGATGCTGAAA	Forward primer to amplify *sal* for CRISPR-Cas9 invitro cleavage assay
10.	Sal_CRISPR_Seq_R	TTCATTTAGGGACGGTGGAG	Reverse primer to amplify *sal* for CRISPR-Cas9 invitro cleavage assay
11.	Sal_CRISPR_Guide	GAAATTAATACGACTCACTATAGGTGATCGAGCCGGCGTTGAGTTTTAGAGCTAGAAATAGC	Forward primer for guide synthesis to knockout *sal*
12.	Optix_CRISPR_Guide_1	GAAATTAATACGACTCACTATAGGGGCTTCGCAGCGCTCCAGCTGTTTTAGAGCTAGAAATAGC	Forward primer 1 for guide synthesis to knockout *optix*
13.	Optix_CRISPR_Guide_2	GAAATTAATACGACTCACTATAGGTTCTTCGTCGGGTTCGGGTAGTTTTAGAGCTAGAAATAGC	Forward primer 2 for guide synthesis to knockout *optix*
14.	Dpp_CRISPR_Guide	GAAATTAATACGACTCACTATAGGGAGACTGTTGTTGTACGACGTGGGTTTTAGAGCTAGAAATAGC	Forward primer for guide synthesis to knockout *dpp*
15.	CRISPR_Guide_R	AAAAGCACCGACTCGGTGCCACTTTTTCAAGTTGATAACGGACTAGCCTTATTTTAACTTGCTATTTCTAGCTCTAAAAC	Reverse primer for guide synthesis CRISPR guides
16.	Wg_insitu_F	CAGCAGCTGGATTTTGTCAG	Forward primer to amplify *wg* for in-situ hybridization
17.	Wg_insitu_R	TATTGTGCCGTTGTCATCGT	Reverse primer to amplify *wg* for in-situ hybridization
18.	Sal_qPCR_F	TGTATGCCATCGCGTATTGT	Forward primer to amplify *sal* for qPCR
19.	Sal_qPCR_R	TAGTGGTAAACGCACGACCA	Reverse primer to amplify *sal* for qPCR
20.	FK506_qPCR_F	AAACTAACCTGCAGCCCTGA	Forward primer to amplify FK506 for qPCR
21.	FK506_qPCR_R	CAAGACGGAGAAGTTCCACA	Reverse primer to amplify FK506 for qPCR
22.	UBQL40_qPCR_F	CGGTAAACAATTGGAAGATGG	Forward primer to amplify UBQL40 for qPCR
23.	UBQL40_qPCR_R	CGAAGTCTGAGGACAAGATGC	Reverse primer to amplify UBQL40 for qPCR

Table S2. Spalt CRISPR-Cas9 injection table

Sl. No.	Concentration	Date	Eggs Injected	Hatchlings	% Hatchlings
1.	300 ng/µl	28th Sept 2018	302	48	15.9
2.	300 ng/µl	10th Oct 2018	306	25	8.2
3.	300 ng/µl	11th Nov 2018	120	18	15.0
4.	300 ng/µl	9th Feb 2019	135	8	5.9

Table S3. Optix CRISPR-Cas9 injection table

Sl. No.	Concentration	Date	Eggs Injected	Hatchlings	% Hatchlings
1.	300 ng/µl	11th March 2020	785	85	10.8
2.	300 ng/µl	12th March 2020	398	47	11.9
3.	300 ng/µl	6th June 2020	326	65	19.9

Table S4. Dpp CRISPR injection table

Sl. No.	Concentration	Date	Eggs Injected	Hatchlings	% Hatchlings
1.	300 ng/µl	23rd Jan 2020	623	89	14.3
2.	300 ng/µl	3rd Mar 2020	923	117	12.7
3.	300 ng/µl	11th Mar 2020	427	64	14.9

Table S5. *In-situ* hybridization Buffers

Buffers	Chemicals	Amount
10X PBS (500 ml) * Sterilize by autoclaving.	K_2HPO_4	5.34 g
	KH_2PO_4	2.64 g
	NaCl	40.9 g
	DEPC treated H_2O	To 500 ml
1X PBST (50 ml)	1X PBS	50 ml
	Tween® 20	50 µl
20X SSC (1000 ml) *Adjust the pH to 7.0 with 1M HCl and sterilize by autoclaving.	NaCl	175.3 g
	Trisodium citrate	88.2 g
	DEPC treated H_2O	Till 1000 ml
Pre-hybridization buffer (40 ml)	Formamide	20 ml
	20X SSC	10 ml
	DEPC treated water	10 ml
	TWEEN20	40 µl
Hybridization buffer (40 ml)	Formamide	20 ml
	20X SSC	10 ml
	DEPC treated water	10 ml
	TWEEN20	40 µl
	Salmon sperm	40 µl
	Glycine (100mg/ml)	40 µl
Block buffer (50 ml)	1X PBS	50 ml
	TWEEN20	50 µl
	BSA	0.1 gm
Alkaline phosphatase buffer (20 ml)	Tris-HCl (pH 8.0)	2 ml
	NaCl (5M)	400 µl
	$MgCl_2$ (200mM)	250 µl
	DEPC treated water	Till 20 ml
	TWEEN20	20 µl

Table S6. Immunohistochemistry Buffers

Buffers	Chemicals	Amount
Fix buffer (30 ml)	M PIPES pH 6.9 (500 mM)	6 ml
	mM EGTA pH 6.9 (500mM)	60 µl
	% Triton x-100 (20 %)	1.5 ml
	mM $MgSO_4$ (1M)	60 µl
	37% Formaldehyde	55 µl per 500 µl of buffer
	dH_2O	22.4 ml
Block buffer (40 ml)	50 mM Tris pH 6.8 (1 M)	2 ml
	150 mM NaCl (5 M)	1.2 ml
	0.5% IGEPAL (NP40) (20%)	1 ml
	5 mg/ml BSA	0.2 gr
	H2O	35.8 ml
Wash buffer (200 ml)	50mM Tris pH 6.8 (1 M)	10 ml
	150 mM NaCl (5 M)	6 ml
	0.5% IGEPAL (20 %)	5 ml
	1 mg/ml BSA	0.2 gr
	dH_2O	179 ml
Mounting media	Tris-HCl (pH 8.0)	20 mM
	N-propyl gallate	0.5%
	Glycerol	60%

Table S7. Raw Cq data on the Dorsomorphin and DMSO treated samples

Biological replicates	Raw Cq (Dorsomorphin treated)			Raw Cq (DMSO treated)		
	spalt	FK506	UBQL40	*spalt*	FK506	UBQL40
1 (5th July 2019)	28.36	22.50	20.89	28.10	22.69	21.05
	28.36	22.61	20.96	28.05	22.55	20.94
	28.20	22.54	20.76	27.76	22.67	20.94
2 (14th April 2019)	31.54	22.57	20.89	30.43	22.22	20.64
	31.80	22.56	20.90	30.59	22.16	20.47
	31.23	22.50	20.87	30.58	22.19	20.67
3 (21st May 2019)	32.02	22.76	21.15	30.40	22.23	20.60
	31.67	22.72	21.11	30.55	22.16	20.44
	31.39	22.62	21.00	30.32	22.29	20.72

Supplementary Materials and Methods

Peptides used for antibody development (Highlighted in green)

Spalt (XP_023939142.1)

MPRVKPACVRRVSIGESSGSCSEEDVGNAMPDEARDRPEAHMCPRCQEQFENLHDFLYHKRLCDEKAMQM
GEERMHSDPEDMVVSGDEEMDGPNKRLEQVRRHRQDAENNNSLEDGEAEIPEADMPPVGLPFPLAGHVTL
EALQNTRVAVAQFAATAMANNANNEAAIQELQVLHNTLYTLQSQQVFQLQLIRQLQNQLSLTRRKEDDPH
SPPPSEPEQNAPSTPARSPSPPRPPREPSPVIPSPPTSQSLPSTHTHHTPKTEQISIPKIPTSSPSLMTH
PLYSSISSSLASSIITNNDPPPSLNEPNTLEMLQKRAQEVLDNASQGLLANNLADELAFRKSGKMSPYDG

KSGGRNEPFFKHRCRYCGKVFGSDSALQIHIRSHTGERPFKCNVCGSRFTTKGNLKVHFQRHTSKFPHVK
MNPNPVPEHLDKYHPPLLAQLSPGPIPGMPPHPLQFPPGAPAPFPPNLPLYRPPHHDLLPPRPLGDKPLS
HHPLFAMREEQDAPADLSKPSAPSPPRPASDIFKSEPQDEESQRDSSFEETDRISPKREIEDNDIGQDAE
QDRYPSTSPYDDCSMDSKYSNEDQIGRDSPHVKPDPDQPENLSSKTSSISGPISIATGLRTFPSFPLFPH
SPPSSVSSGSLTPFHHHPNSTMDSALTRDPLFYNAILPRPGSNDNSWESLIEITKTSETTKLQQLVDNIN
NKVSDPNECIVCHRVLSCKSALQMHYRTHTGERPFRCKLCGRAFTTKGNLKTHMGVHRIKPPSQLLHQCP
VCHKKFSDPSMLHQHIRLHTGERNNVFFNQFHDNEINSQSLPGSDVTEYNSFHSIPPPIFPTPSTPGDRR
ADSRGTDDESGRDEREPATREFDDEPDIKDRRTSPLSVCASASEFEVKTITTTASLPSATGSESGRSARG
SPPSPSPSPSALSTPPRLPHHSPLPSPPTPLAALGALGGSPFSPLGLAFPPAVRGNTTCTICYKTFACNS
ALEIHYRSHTKERPFKCTVCDRGFSTKSSGGGCQCGRRARAPRPPHATALDLWNAFVYPGNMKQHMLTHK
IRDMPPGFDKGPGGPSGPPSEEGRDPSPDRRSSPEKLDLKRSPPVHPPPPMSHPPIDMPPLPKRPTVPSI
PSHPPPSASSKHLCGVCRKNFSSSSALQIHMRTHTGDKPFRCAVCQKAFTTKGNLKGLLLPATRLISRST
NQATALFGTLGPFIYRLSELYAPPSATSALRLVELSDFGSADFR

Armadillo (XP_023941962.1)

MSYQIPSSQSRTMSHSNYGGSDVPMAPSKEQQTLMWQQNSYLVDSGINSGAATQVPSLTGKEDDEMEGDQ
LMFDLDQGFAQGFTQEQVDDMNQQLSQTRSQRVRAAMFPETLEEGIEIPSTQLDPAQPTAVQRLSEPSQM
LKHAVVNLINYQDDADLATRAIPELIKLLNDEDQVVVSQAAMMVHQLSKKEASRHAIMNSPQMVAALVRA
ISNSNDLETTKGAVGTLHNLSHHRQGLLAIFKSGGIPALVKLLSSPVESVLFYAITTLHNLLLHQDGSKM
AVRLAGGLQKMVALLQRNNVKFLAIVTDCLQILAYGNQESKLIILASQGPIELVRIMRSFDYEKLLWTTS
RVLKVLSVCSSNKPAIVEAGGMQALAMHLGNPSGRLVQNCLWTLRNLSDAATKVEGLEGLLQSLVQVLAS
TDVNIVTCAAGILSNLTCNNQRNKVTVCQAGGVDALVRTVVSAGDREEITEPAVCALRHLTSRHVESEMA
QNAVRLHYGLPVIVKLLQPPSRWPLVKAVVGLVRNLALCPANHAPLREHGAVHHLVRLLLRAFNDTQRQR
GSVSGGGGAGGAYADGVRMEEIVEGAVGALHILAREGLNRALIRQQNVIPIFVQLLFNEIENIQRVAAGV
LCELAADKEGAEMIEAEGATAPLTELLHSRNEGVATYAAAVLFRMSEDKPHDYKKRLSMELTNSLFRDDH
QMWPNDLAMQPDLQDMLGPEQGYEGLYGTRPSFHQQGYDQIPIDSMQGLEIGSGFGMDMDIGEADGGGAA
SADLAFPEPPLDNNNVAAWYDTDL

Rhomboid (XP_023940805.1)

MANQQEHNKRYMSGKRTRSYRCAVHQRDREVSSENDFHLLLEDPTLFARMVHLVAMEVLPEERDRKYYQE
RYTCCPPPFFIICVTLLELGVFAWYAWGAGGVAAAAGPVPVDSPLVYRPDRRRELWRFLTYSVVHAGWLH
LAFNLLVQLAVGLPLEMVHGAVRCGAVYLAGVLGGSLAASVLDPDVCLAGASGGVYALLAAHLANALLNF
HAMRYGAVRLVAALAVASCDVGFAVHARYTKQEAPPVSYAAHVAGALAGLTIGLLVLKHAQQRLWERLLW
WAALGAYAACTLFAVLYNVFSAPVDELHYMPPDPPPDAGF

Sequences

Sequence of *engrailed* used for *in-situ* hybridization (XM_024092264.1)

TTGAAGACCGTTGCAGTCCGAACCAGGCCAACAGCCCCGGTCCGGTCACCGGCAGAGTCCCTGCGCCTCA
CTCCGAAGTAAGAAACGNGTACCAAAGTCAATACACTTGCACGACTATCGATCAAAGGTTTGACAGAACG
ATGACAGTGGTGAAAGTGCAGCCGAATTCACCACCGATGAGTCCACTGACGTGAAGCCCATAATCCCTGA
GTTTGAAGACAAGAGAAACCGACAACCACCACCAACCATACCCTTCTCTATCAGCAACATATTACACCCA
GAATTCGGTTTGACAGCGATTCGAAAAACGAACAAAATCGAAGGACCAAAACACGTCGGCCCCAACCACA
GCATTTTGTACAAACCTTATTTGTCGAACGAGTTATCGAGTTCGAAATTCAATTTCGATTATTTAAAATC
TAAGGATGATTTCGGTGCATTACCTCCACTTGGCGGTTTGAGGCAGACCGTGTCGAATATTGGAGAACAG
AAGGAGGCACCAAAGATTATAGAGCAGCAGAAGAGGCCAGATTCAGCCAGCTCTATTGTCTCTTCCACAT
CTAGCGGGGCTTTATCGACGTGTGGCAGCACTGACGCCAACAGCAGTCAAAGCGGGAACAGCAATCTA

Sequence of *invected* used for *in-situ* hybridization (XM_024092263.1)

GGACCAAAGTGACGAAGAGCACGACCCCTACTCGCCCAACACTAGAGACACCATCACACCAGACTTCATA
GAAGAAGACAAACAAGACAGGCCTATACACACATCCTCTTTCTCCATACACAATGTCCTTAAGAAGGAAA
GAGACAGTAATAGTCCTGAGAACGTCTTCTCAACTGAAAAGTTGTTGCAAAGTACACCGAACTTTGAAGA
TTCTAGGAACTCTGAAAGCGTTAGTCCGAGACTTGAAGATGATCACAATGAAAGAGCTGATATAAGTGTT

GATGACAACTCTTGTTGTAGTGATGATACTGTGCTATCTGTTGGCAATGAAGCCTTACCAACCAATTACC
CAAACGACAAAGATCCGAACCAAGGCTTAACCTCCTTCAAACATATACAAACTCATTTGAACGCAATATC
ACAGTTAAGTCAAAATTTAAACATAAACCAACCAATCCTCCTACGACCCAACCCAATAACACCAAACCCG
TTAATGTTCCTAAACCAACCGTTGTTATTCCAAAACCCTTTAATAAACCAAGTGGATTTAAAATCAGGGT
TACCGAGAATCGGCTTGCAGCAAAACAATTTAAATTTGAACCAAAATTACATGAATTATGCGAGAAAAAA
TGAACTGAACGAAAGACGACAGAGTTATTCACCGAAGTTACATGAAAATGAGTCAAGTAGAGATTTTATT
AACCAAGGATGTTTGAAATTTAGCATTGATAATATACTGAAAGCTGATTTTGGTAGACGAATTACTGATC
CGTTGACAAAGAGAAAAACGAAGACGAGGCAGTATGAGGCAAAATCTACCCCTGTCAAAGAGGTTCAGTC
TCCCCCTAAAGAGGTAGAGGCTAGAGTGCCGGA

Sequence of *decapentaplegic* used for *in-situ* hybridization (XM_024080858.1)

GTTCTTCAACGTAAGCGGCGTACCGGCCGACGAGGTGGCGCGCGGCGCCGACCTCTCGTTCCAACGAGCC
GTCGGCACCACCGGCAGACAGAGACTGTTGTTGTACGACGTGGTGCGCCCTGGCCGCCGCGGCCACTCCG
AGCCGATCCTGCGGCTGCTGGACTCCGTTCCGCTCCGGCCCGGGGAGGGAATCGTCAACGCCGACGCTCT
GGGAGCGGCGCGACGGTGGCTCAAAGAGCCCAAACATAATCACGGACTATTAGTGCGAGTGTTAGAAGAA
GACGCCGCGAGTGCGAGCAGGGACGCGAAGTTCCCGCACGTGCGCGTGCGCAGACGCGTCACGGACGAGG
AGGAGGAGTGGCGGACGGCGCAGCCGCTGCTCATGCTGTACACGGAGGACGAGCGCGCGCGCGCGTCGCG
GGAGACGAGCGAGCGGCTGACGCGCAGCAAGCGCGCGGCGCAGCGGCGGGGGCACCGCGCGCACCACCGC
CGCAAGGAGGCGCGCGAGATCTGCCAGCGCCGCCCGCTGTTCGTCGACTTCGCGGACGTGGGCTGGAGCG
ACTGGATCGTGGCCCCGCACGGCTACGACGCGTACTACTGCCAGGGCGACTGCCCCTTCCCGCTGCCGGA
CCACCTCAACGGCACGAACCACGCGATAGTGCAGACTCTGGTCAACTCAGTGAACCCCGCGACGGTGCCC
AAAGCGTGCTGCGTGCCGACGCAACTCTCATCTATATCTATGTTATATATGGACGAAGTGAACAATGTGG
TGCTTAAAAACTATCAGGACATGATGGTGGTAGGCTGTGG

Sequence of *blistered* used for *in-situ* hybridization (XM_024084428.1)

GCATACGAGCTATCAACGCTGACCGGCACCCAAGTGATGCTGCTGGTCGCGTCGGAGACCGGCCACGTGT
ACACGTTCGCGACACGCAAACTGCAGCCGATGATCACGTCCGACTCGGGCAAGCGGCTCATACAGACGTG
CCTCAACTCGCCCGACCCGCCCACCACCAGCGAGCAGCGCATGGCCGCCACCGGCTTCGAGGAGACCGAG
CTCACGTATAACGTTGTAGACGACGAGATGAAGGTGAGACAACTGGCGTACGCTAACCAGTACCCCATAG
AGCACCACCCGGGGTTGGCGCCGTCGCCACTGCAGCAGTACCACCAGCACCCGCCCTGCCCCTCGCCCCT
CCCCCTCGGCTCGCTGGGCCAGCCGTACTCGCACGCGCATCTATCGCACCCCCACATGTCTCACCACCCG
CAACG

Sequence of *wingless* used for *in-situ* hybridization (XM_024099417.1)

CAGCAGCTGGATTTTGTCAGTCCAGCTAGGAAGGGGGGCATAGCAAAGGCAGGCGAACCAAATAACTTAT
CACCCTTGTCTCCAAGTGTCCTATACATGGACCCGGCTGTTCACGCCACCTTGAGGAGGAAACAGAGAAG
GCTAGCGAGGGAGAACCCTGGGGTCCTCGCAGCAATATCCAAGGGAGCCAGCATGGCTGTGGCCGAATGC
CAGCATCAGTTCAAATACAGGAGATGGAACTGTTCTACAAGAAATTTTTTGCGAGGGAAGAATCTATTTG
GAAAAATTGTTGACAGAGTTTCGCCGGACAAAGCCCCCCCGGCCGGGGCGGCTATAATTACTAATATACA
CGTCGACACGCCATTGACGATTGACGCGACATCTTCATTTCATTGTGGTGTAAACCTCAAGGATCGCATT
AACACGGACGATGACAACGGCACAATA

CRISPR targets

Region of *spalt* targeted by CRISPR-Cas9 (location of guide RNA highlighted in red) (XM_024083374.1)

GCATCGACAAGATGCTGAAAATAATAATAGTCTCGAAGACGGCGAGGCCGAAATACCTGAAGCCGACATG
CCCCCCGTGGGTCTGCCGTTCCCTTTGGCAGGACACGTTACTCTTGAGGCTCTACAAAATACGAGAGTAG
CGGTCGCCCAATTCGCTGCAACAGCGATGGCAAATAATGCGAATAACGAAGCTGCTATACAAGAATTACA
AGTGTTACACAACACTCTATACACTTTACAGTCACAACAAGTATTTCAACTTCAGTTAATACGTCAGCTT
CAGAATCAGTTATCTCTAACTCGACGGAAAGAAGACGATCCACACAGCCCACCGCCAAGTGAACCAGAAC
AGAATGCCCCGTCAACGCCGGCTCGATCACCGTCGCCGCCGCGTCCGCCACGGGAGCCGTCGCCTGTTAT
ACCCTCTCCTCCTACTAGCCAAAGTTTGCCGTCGACTCACACACATCACACACCCAAAACTGAACAGATA

TCTATCCCTAAGATTCCAACTTCCTCACCATCTTTAATGACCCACCCACTTTATAGTTCAATTTCTTCGT
CATTAGCATCTTCCATCATAACAAACAATGATCCTCCACCGTCCCTAAATGAA

Region of *optix* targeted by CRISPR-Cas9 (location of guide RNAs highlighted in red)
(XM_024080404.1)

ATGCGCGGCTCCTGGGACGAGTCCACGACGGCGGCGCTGCACGCGCGCATCCTGGAGGCGCACCGCGGGT
CCGCCGCGCCCGACCGCGCCGAGCCCGCGTGCGAGCCTCCGCCGCTGACGCTGGGCGCGCTGGAGCTGGC
GGCGCCCACGCCGCTGCTGCCGCTGCCCACGCTGAGCTTCAGCGCCGCGCAGGTGGCCACCGTGTGCGAG
ACGCTGGAGGAGAGCGGCGACGTGGAGCGCCTGGCGCGCTTCTTGTGGTCGCTGCCCGTGGCGCACCCCA
ACGTGGCCGAGCTGGAGCGCTGCGAAGCCGTGCTGCGCGCGCGCGCCGTCGTCGCCTTCCACGCCGGCCG
CCACCGCGAGCTGTACGCCATCCTCGAGCGCCACCGCTTCCAGCGCTCCAGCCACGCCAAGCTGCAAGCG
CTGTGGCTGGAGGCGCACTACCAGGAGGCTGAGCGCCTGCGCGGCCGTCCGCTGGGCCCCGTCGACAAGT
ACCGCGTGCGGAAGAAGTTCCCGCTCCCGAGGACGATCTGGGACGGCGAGCAGAAGACGCACTGTTTCAA
GGAGCGGACGCGATCTCTACTCCGAGAATGGTACCTCCAAGATCCCTACCCGAACCCGACGAAGAAGAGG
GAATTGGCGGCGGCGACGGGTCTGACGCCGACGCAAGTCGGCAACTGGTTCAAAAACCGACGGCAAAGAG
ACCGAGCGGCCGCCGCCAAGAACCGCTCCGCCGTGCTGGGCAGAGGATAA

Region of *dpp* targeted by CRISPR-Cas9 (location of guide RNA highlighted in red)
(XM_024080858.1)

GTTCTTCAACGTAAGCGGCGTACCGGCCGACGAGGTGGCGCGCGGCGCCGACCTCTCGTTCCAACGAGCC
GTCGGCACCACCGGCAGACAGAGACTGTTGTTGTACGACGTGGTGCGCCCTGGCCGCCGCGGCCACTCCG
AGCCGATCCTGCGGCTGCTGGACTCCGTTCCGCTCCGGCCCGGGGAGGGAATCGTCAACGCCGACGCTCT
GGGAGCGGCGCGACGGTGGCTCAAAGAGCCCAAACATAATCACGGACTATTAGTGCGAGTGTTAGAAGAA
GACGCCGCGAGTGCGAGCAGGGACGCGAAGTTCCCGCACGTGCGCGTGCGCAGACGCGTCACGGACGAGG
AGGAGGAGTGGCGGACGGCGCAGCCGCTGCTCATGCTGTACACGGAGGACGAGCGCGCGCGCGCGTCGCG
GGAGACGAGCGAGCGGCTGACGCGCAGCAAGCGCGCGGCGCAGCGGCGGGGGCACCGCGCGCACCACCGC
CGCAAGGAGGCGCGCGAGATCTGCCAGCGCCGCCCGCTGTTCGTCGACTTCGCGGACGTGGGCTGGAGCG
ACTGGATCGTGGCCCCGCACGGCTACGACGCGTACTACTGCCAGGGCGACTGCCCCTTCCCGCTGCCGGA
CCACCTCAACGGCACGAACCACGCGATAGTGCAGACTCTGGTCAACTCAGTGAACCCCGCGACGGTGCCC
AAAGCGTGCTGCGTGCCGACGCAACTCTCATCTATATCTATGTTATATATGGACGAAGTGAACAATGTGG
TGCTTAAAAACTATCAGGACATGATGGTGGTAGGCTGTGG